NATIONAL ADVISORY COMMITTEE FOR AERONAUTICS

TECHNICAL NOTE 4069

EFFECT OF ANGLE OF ATTACK AND THICKNESS ON AERODYNAMIC COEFFICIENTS OF A RIGID WING OSCILLATING AT VERY LOW FREQUENCIES IN TWO-DIMENSIONAL SUPERSONIC FLOW

By Frank S. Malvestuto, Jr., and Julia M. Goodwin

Langley Aeronautical Laboratory
Langley Field, Va.

Washington
January 1958

NATIONAL ADVISORY COMMITTEE FOR AERONAUTICS

TECHNICAL NOTE 4069

EFFECT OF ANGLE OF ATTACK AND THICKNESS ON AERODYNAMIC COEFFICIENTS OF A RIGID WING OSCILLATING AT VERY LOW FREQUENCIES IN TWO-DIMENSIONAL SUPERSONIC FLOW

By Frank S. Malvestuto, Jr., and Julia M. Goodwin

SUMMARY

Analytical expressions are presented for the lift and pitching-moment coefficients of a wing of finite thickness performing a plunging motion and rotary oscillations about some fixed angle of attack at very low frequencies in two-dimensional flow.

Calculated lift and pitching-moment coefficients are presented for the entire range of angle of attack and thickness for which the flow behind the shock attached to the leading edge is everywhere supersonic, although the effect of viscous separation at the finite angles of attack restricts the validity of the results to a much smaller range of these parameters.

Design charts are presented which permit rapid calculations to be made of the aerodynamic coefficients for a given Mach number, angle of attack, and thickness. In addition, some illustrations are included for the effect of angle of attack and thickness on the neutral-stability boundary for slowly oscillating wings.

The results of the analysis and calculations show that for the flat-plate section and wedge section of finite thickness, increasing Mach number, for a fixed angle of attack of the wing, decreases the positive (destabilizing) values of the pitching-moment derivative $c_{m_q} + c_{m_{\dot{\alpha}}}$ and eventually causes the values of the derivative to become negative (stabilizing). For a fixed Mach number, increasing the angle of attack of the wing in the moderate and high angle-of-attack range decreases the negative value of the pitching-moment derivative. This effect becomes more predominant with increasing wedge thickness and rearward movements of the pitching-axis location.

INTRODUCTION

In recent years considerable effort has been expended toward the theoretical calculation of the aerodynamic loads, forces, and moments acting on oscillating wings in the supersonic speed range. For wings with little or no thickness at low angles of attack, the calculation of the aerodynamic coefficients is based upon linearized potential-flow theory. For a wing with finite thickness in two-dimensional flow and at an angle of attack where the flow behind the leading-edge shock (shock attached to leading edge) is rotational, the application of inviscid linearized rotational-flow theory permits the evaluation of the aerodynamic coefficients.

Considerable information is now available on the effect of angle of attack and thickness on the aerodynamic coefficients of a wing oscillating at very low frequencies in two-dimensional flow, but this information is scattered throughout the literature. The object of the present paper is to present a collection of most of the pertinent information together with fairly extensive evaluations of certain formulas. In addition, it should be pointed out that all expressions for the aerodynamic coefficients considered in this paper have been independently checked, and some additional expressions are derived by extensions of available formulas.

The information presented herein covers the effect of angle of attack on the loads, forces, and moments of a wing performing a plunging motion and rotary oscillations at very low frequencies in two-dimensional flow. In addition, the effect of thickness on the aerodynamic coefficients has been studied through the application of the theory to a wing with a wedge airfoil section. The results are valid for a range of Mach number and angle of attack for which the flow behind the leading-edge shock is everywhere supersonic. (The shock must be attached to the leading edge.)

The reader should be cautioned, however, that the effect of viscous separation at finite angles of attack of the wing probably restricts the validity of the results of the analysis to a much smaller range of these parameters. Some qualitative indications of the effect of viscosity on unsteady-flow behavior for oscillating wings can be found in reference 1.

SYMBOLS

$$a = \frac{1 + K_{II}}{M_1^2\gamma(\gamma - 1)}$$

$B_1 = \sqrt{M_1^2 - 1}$

$B_2 = \sqrt{M_2^2 - 1}$

$C_{p,l}$ pressure coefficient of lower surface of airfoil, $\frac{p_1 - p_\infty}{\frac{1}{2}\rho_\infty V_\infty^2}$

$C_{p,u}$ pressure coefficient of upper surface of airfoil, $\frac{p_2 - p_\infty}{\frac{1}{2}\rho_\infty V_\infty^2}$ for $\alpha_o > |\delta|$, and $\frac{p_1 - p_\infty}{\frac{1}{2}\rho_\infty V_\infty^2}$ for $\alpha_o < |\delta|$

ΔC_p pressure difference, $C_{p,l} - C_{p,u}$

c wing chord

c_l lift coefficient, $c_n \cos \alpha_o$

$$c_{l_q} = \left(\frac{\partial c_l}{\partial \frac{qc}{2V_\infty}}\right)_{\alpha=\alpha_o} = c_{n_q} \cos \alpha_o$$

$$c_{l_\alpha} = \left(\frac{\partial c_l}{\partial \alpha}\right)_{\alpha=\alpha_o} = c_{n_\alpha} \cos \alpha_o$$

$$c_{l_{\dot{\alpha}}} = \left(\frac{\partial c_l}{\partial \frac{\dot{\alpha}c}{2V_\infty}}\right)_{\alpha=\alpha_o} = c_{n_{\dot{\alpha}}} \cos \alpha_o$$

c_m pitching-moment coefficient, $\frac{\text{Pitching moment}}{\frac{1}{2}\rho_\infty V_\infty^2 c^2}$

$$c_{m_q} = \left(\frac{\partial c_m}{\partial \frac{qc}{2V_\infty}}\right)_{\alpha=\alpha_o}$$

$$c_{m_{\dot{\alpha}}} = \left(\frac{\partial c_m}{\partial \frac{\dot{\alpha}c}{2V_\infty}}\right)_{\alpha=\alpha_o}$$

c_n normal-force coefficient, $\frac{\text{Normal force}}{\frac{1}{2}\rho_\infty V_\infty^2 c}$

$c_{n_q} = \left(\frac{\partial c_n}{\partial \frac{qc}{2V_\infty}}\right)_{\alpha=\alpha_o}$

$c_{n_\alpha} = \left(\frac{\partial c_n}{\partial \alpha}\right)_{\alpha=\alpha_o}$

$c_{n_{\dot{\alpha}}} = \left(\frac{\partial c_n}{\partial \frac{\dot{\alpha}c}{2V_\infty}}\right)_{\alpha=\alpha_o}$

$K_I a$ flow parameter defined by equation (3)

K_{II} flow parameter defined by equation (7)

K_{III} flow parameter defined by equation (16)

M_1 Mach number behind shock in unperturbed flow

M_2 Mach number behind expansion fan in unperturbed flow

M_∞ free-stream Mach number

m slope of shock, $\tan \beta$

p_1 pressure behind shock in unperturbed flow

p_2 pressure behind expansion fan in unperturbed flow

p_∞ free-stream pressure

q steady pitching angular velocity

t maximum thickness of airfoil section, $2c \tan |\delta|$

V_1 velocity behind shock in unperturbed flow

V_∞ free-stream velocity

x,z rectangular coordinates (see fig. 1)

$\bar{x}$ x-coordinate of pitching axis measured parallel to wing chord plane of symmetry

α angle of attack

α_o fixed angle of attack of airfoil

$\dot{\alpha}$ rate of change of wing angle of attack with time

$\beta = \theta - \epsilon$

γ ratio of specific heats

δ semiapex angle of wedge section

ϵ inclination of airfoil surface to free-stream direction

ϵ_l acute angle between free-stream direction and lower surface of airfoil, $\alpha_o + |\delta|$

ϵ_u acute angle between free-stream direction and upper surface of airfoil, $\alpha_o - |\delta|$

θ acute angle between free-stream direction and steady-flow shock direction

$\xi = \frac{\bar{x}}{c}$

ρ_1 density behind shock in unperturbed flow

ρ_2 density behind expansion fan in unperturbed flow

ρ_∞ free-stream density

Superscripts:

q pitching angular velocity

α angle of attack

$\dot{\alpha}$ constant vertical acceleration

PRELIMINARY REMARKS

Sketches of the wing in two-dimensional flow, the coordinate-axis system employed herein, and the positive direction of the lift and pitching moments are presented in figure 1. The left-hand sketch of figure 1(a) shows the flat-plate wing section that is used to determine the effect of angle of attack on the aerodynamic coefficients. In the right-hand side of figure 1(a) is a sketch of a wing with a wedge cross section, and it is this distribution of thickness that is used to evaluate the effect of thickness on the aerodynamic coefficients at zero and finite angles of attack.

The results of the analysis, presented in terms of aerodynamic coefficients, are valid for the range of Mach number and angle of attack for which the leading- and trailing-edge shocks remain attached to their respective edges, provided viscous effects are neglected. Variation of the maximum inclination of the lower surface at which the shock still remains attached with free-stream Mach number is given by the curves in figure 2 for the flat-plate and wedge sections.

Aerodynamic Coefficients and Wing Motions

Harmonically oscillating wings lead to a natural resolution of the aerodynamic forces and moments into in-phase components that depend upon the instantaneous angle of attack and into out-of-phase components that depend upon instantaneous rate of change of angle of attack.

The primary interest herein is the evaluation of the out-of-phase components of the oscillatory lift and pitching-moment coefficients acting on a wing performing rotary oscillations at very low frequencies in two-dimensional flow. These aerodynamic quantities from a flutter standpoint represent only an approximation, to the first order in frequency, of the total out-of-phase oscillatory coefficients so important in flutter studies. For stability investigations, the derivatives of these first-order lift and pitching-moment coefficients with respect to the variable defining the motion are very important and are generally known as stability-damping derivatives. The final expressions for the aerodynamic coefficients presented herein are in the derivative form.

The damping or out-of-phase forces and moments acting on an airfoil oscillating in pitch may be given to the first order in frequency by the sum of the forces and moments acting on the airfoil performing plunging and steady pitching motions. This fact is demonstrated by the following derivation of the angle-of-attack distribution to the first order in frequency on a flat-plate airfoil oscillating in pitch about $\alpha = 0$. The symbol notation is clarified by the accompanying sketch:

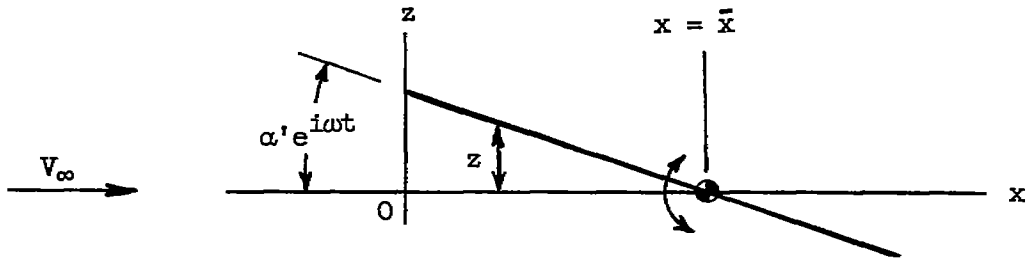

The vertical displacement of any point on the wing which is performing small sinusoidal pitching oscillations of small amplitude α' and frequency ω about an axis located at $x = \bar{x}$ is given by

$$z = \alpha' e^{i\omega t}(x - \bar{x})$$

The vertical velocity w on the surface is

$$w = V_\infty \alpha' e^{i\omega t} + i\omega\alpha'(x - \bar{x})e^{i\omega t}$$

Expanding $e^{i\omega t}$ and neglecting the terms of higher order in ω than the first results in

$$w = V_\infty \alpha' + i\left[\omega V_\infty \alpha' t + \omega\alpha'(x - \bar{x})\right]$$

To the order of the approximations stated, the first term in the out-of-phase bracket is the increment of the total downwash at any point x produced as a result of the vertical acceleration associated with this point when the airfoil undergoes an oscillatory rotation about $x = \bar{x}$ (plunging effect). In the same sense, the second term in the bracket can be thought of as the increment of the total downwash at the point x due to a steady rotation of the wing about the point $x = \bar{x}$ (steady pitching or camber effect). This steady-rotation downwash increment results, as does the vertical-acceleration downwash increment, from the first-order approximation to the oscillatory rotary motion about $x = \bar{x}$.

If in the preceding expression w is divided by V_∞, and ω is set equal to q/α' or $\dot{\alpha}/\alpha'$, the following expression is obtained for the local angle of attack:

$$\alpha_{local} = \alpha' + i\left[\dot{\alpha}t + \frac{q}{V_\infty}(x - \bar{x})\right]$$

It is now clear that the out-of-phase terms in α_{local} are the angles of attack due to plunging and steady pitching, as indicated previously.

Theoretical Considerations

Some of the considerations employed in the analytical developments are available for evaluating the aerodynamic coefficients of the wing and are now summarized briefly. Full developments of the analyses are not warranted since they may be found in references 2 to 5.

Along the upper surface of the airfoil, behind the expansion fan from the leading edge of the wing and ahead of the strong shock wave from the trailing edge, the basic unperturbed flow is irrotational. The perturbed flow resulting from movements of the wing is also irrotational since any perturbations of the trailing-edge shock do not produce flow changes in the wing field. For the upper surface of the airfoil, then, it is a simple process to evaluate the pressures that give rise to the aerodynamic coefficients by an application of linearized supersonic-flow theory. This procedure was carried out in reference 4, and in that paper expressions are presented for the pressures for the various motions.

Along the lower surface of the wing the unperturbed flow behind the shock from the leading edge is rotational. It is possible, however, to determine analytically the pressure distribution along the lower surface for time-dependent motions of the wing by a linearization of the equations of rotational flow, together with a knowledge of the boundary values of the perturbed-flow variables along the attached shock surface and wing surface. Full details of the linearization process for the time-dependent flow equations are given by Carrier in reference 5.

FORMULAS FOR PRESSURES, FORCES, AND MOMENTS

Forces and Moments Produced by an Incremental Change From a Finite Angle of Attack

The aerodynamic coefficients associated with an incremental change in angle of attack have been given in reference 4. These coefficients are reproduced here for the sake of completeness and for use in later developments.

Flat-plate section.- The pressure difference in coefficient form $\Delta C_p{}^{\alpha}$ produced by an incremental change $\Delta\alpha$ in angle of attack is

$$\Delta C_p{}^{\alpha} = C_{p,l} - C_{p,u} = -\Delta\alpha \frac{2}{M_\infty{}^2}\left(M_1{}^2 \frac{p_1}{p_\infty} K_I a - \frac{M_2{}^2}{B_2} \frac{p_2}{p_\infty}\right)_{\epsilon=\alpha_0} \qquad (1)$$

The corresponding expression for the lift coefficient in derivative form is

$$c_{l_\alpha} = \frac{\partial c_l}{\partial \Delta\alpha} = -\frac{2}{M_\infty^2}\left(M_1^2 \frac{p_1}{p_\infty} K_I a - \frac{M_2^2}{B_2}\frac{p_2}{p_\infty}\right)_{\epsilon=\alpha_0} \cos \alpha_0 \qquad (2)$$

The pressure ratios p_1/p_∞ and p_2/p_∞ as functions of M_∞ and α_0 are determined from the following relations presented in reference 6:

$$\frac{p_1}{p_\infty} = 1 + \frac{\gamma M_\infty^2}{\left(M_\infty^2 - 1\right)^{1/2}}\epsilon + \gamma M_\infty^2 \frac{(\gamma+1)M_\infty^4 - 4\left(M_\infty^2 - 1\right)}{4\left(M_\infty^2 - 1\right)^2}\epsilon^2 + \frac{\gamma M_\infty^2}{\left(M_\infty^2 - 1\right)^{7/2}}\left[\frac{(\gamma+1)^2}{32}M_\infty^8 - \frac{7 + 12\gamma - 3\gamma^2}{24}M_\infty^6 + \frac{3}{4}(\gamma+1)M_\infty^4 - M_\infty^2 + \frac{2}{3}\right]\epsilon^3 + \cdots$$

$$\frac{p_2}{p_\infty} = 1 - \frac{\gamma M_\infty^2}{\left(M_\infty^2 - 1\right)^{1/2}}\epsilon + \gamma M_\infty^2 \frac{(\gamma+1)M_\infty^4 - 4\left(M_\infty^2 - 1\right)}{4\left(M_\infty^2 - 1\right)^2}\epsilon^2 - \frac{\gamma M_\infty^2}{2\left(M_\infty^2 - 1\right)^{7/2}}\left[\frac{\gamma+1}{6}M_\infty^8 - \frac{5 + 7\gamma - 2\gamma^2}{6}M_\infty^6 + \frac{5}{3}(\gamma+1)M_\infty^4 - 2M_\infty^2 + \frac{4}{3}\right]\epsilon^3 + \cdots$$

where ϵ in $\frac{p_1}{p_\infty}$ and $\frac{p_2}{p_\infty}$ is replaced by α_0 when substituted into equations (1) and (2). The quantity $K_I a$ has been previously derived in references 4 and 7. This quantity is compactly defined as follows in terms of θ, M_∞, and ϵ:

$$K_I a = -\frac{2M_\infty^2 \sin^2(\theta - \epsilon)\sin^2\theta}{\left(1 + M_\infty^2\sin^2\theta\right)\cos(\theta - \epsilon) + \left(1 - M_\infty^2\sin^2\theta\right)\tan\theta\,\sin(\theta - \epsilon)} \qquad (3)$$

where θ is the angle of the unperturbed leading-edge shock relative to the free-stream direction. (See fig. 3.) As in the case of the pressure ratios, ϵ is replaced by α_0 when substituted into equations (1)

and (2). For convenience, $K_I a$ has been plotted against ϵ in figure 4 for a range of free-stream Mach numbers M_∞. Illustrative variations of c_{l_α} with angle of attack for several Mach numbers are presented in reference 4.

Wedge section.- Determining the expressions for the pressure due to the lifting motion and lift coefficient for the wedge airfoil section is a simple process once these expressions are available for the flat-plate airfoil section (or wedge section at zero angle of attack). In figure 3 it is seen that the angle of inclination of the lower surface is $\epsilon_l = \alpha_o + |\delta|$ and that the angle of inclination of the upper surface of the wedge is $\epsilon_u = \alpha_o - |\delta|$ where $|\delta|$ is the absolute value of the semiapex angle of the wedge. Below the wing, the flow parameters are M_1, p_1, and ρ_1 and depend upon the shock-flow turning angle $\epsilon_l = \alpha_o + |\delta|$; above the wing when $\alpha_o > |\delta|$, the flow parameters are M_2, p_2, and ρ_2 and depend upon the expansion angle $\epsilon_u = \alpha_o - |\delta|$. For $\alpha_o < |\delta|$, the flow over the upper surface is not expanded but compressed; that is, the upper surface has an attached leading-edge shock, and the flow parameters are M_1, p_1, and ρ_1 and are functions of the shock-flow turning angle $\epsilon_u = |\delta| - \alpha_o$. The expressions for the pressure due to the lifting motion in coefficient form are

$$\Delta C_p{}^{\alpha} = C_{p,l}{}^{\alpha} - C_{p,u}{}^{\alpha}$$

$$\Delta C_p{}^{\alpha} = -\Delta\alpha \frac{2}{M_\infty{}^2}\left[\left(M_1{}^2 \frac{p_1}{p_\infty} K_I a\right)_{\epsilon=\epsilon_l} - \left(\frac{M_2{}^2}{B_2} \frac{p_2}{p_\infty}\right)_{\epsilon=\epsilon_u}\right] \qquad (\alpha_o > |\delta|) \qquad (4a)$$

$$\Delta C_p{}^{\alpha} = -\Delta\alpha \frac{2}{M_\infty{}^2}\left[\left(M_1{}^2 \frac{p_1}{p_\infty} K_I a\right)_{\epsilon=\epsilon_l} + \left(M_1{}^2 \frac{p_1}{p_\infty} K_I a\right)_{\epsilon=-\epsilon_u}\right] \qquad (\alpha_o < |\delta|) \qquad (4b)$$

The lift coefficients in derivative form corresponding to equations (4) are

$$c_{l_\alpha} = -\frac{2}{M_\infty{}^2}\left(M_1{}^2 \frac{p_1}{p_\infty} K_I a\right)_{\epsilon=\epsilon_l} \cos(\alpha_o + |\delta|) + \frac{2}{M_\infty{}^2}\left(\frac{M_2{}^2}{B_2} \frac{p_2}{p_\infty}\right)_{\epsilon=\epsilon_u} \cos(\alpha_o - |\delta|)$$

$$(\alpha_o > |\delta|) \qquad (5a)$$

$$c_{l_\alpha} = -\frac{2}{M_\infty^2}\left(M_1^2 \frac{p_1}{p_\infty} K_I a\right)_{\epsilon=\epsilon_l} \cos(\alpha_o + |\delta|) - \frac{2}{M_\infty^2}\left(M_1^2 \frac{p_1}{p_\infty} K_I a\right)_{\epsilon=-\epsilon_u} \cos(|\delta| - \alpha_o)$$

$$(\alpha_o < |\delta|) \qquad (5b)$$

where the subscripts on the parentheses indicate the value of ϵ for which M_1, M_2, $\frac{p_1}{p_\infty}$, $\frac{p_2}{p_\infty}$, and $K_I a$ are to be determined.

Forces and Moments Produced by Constant Vertical Acceleration

Flat-plate section.- The pressure difference in coefficient form $\Delta C_p^{\dot{\alpha}}$ produced by a wing moving downward with an infinitesimal constant acceleration in two-dimensional flow is given by

$$\Delta C_p^{\dot{\alpha}} = \Delta C_{p,l}^{\dot{\alpha}} - \Delta C_{p,u}^{\dot{\alpha}} = -\frac{4}{M_\infty}\frac{\dot{\alpha}c}{2V_\infty}\left(-M_1\sqrt{\frac{p_1\rho_1}{p_\infty\rho_\infty}}\,K_{II} + \frac{M_2}{B_2^3}\sqrt{\frac{p_2\rho_2}{p_\infty\rho_\infty}}\right)_{\epsilon=\alpha_o}\frac{x}{c} \qquad (6)$$

The quantity K_{II} which in the present notation may be written as

$$K_{II} = \frac{\frac{1}{2}\sin 2\beta - K_I a\left(1 + 2\cos^2\beta\right) - \frac{(K_I a)^2 \cot\beta}{M_\infty^2 \sin^2\theta} + (K_I a)^2 \cot\beta\left[B_1^2 \sin^2\beta\left(1 - \frac{2M_1^2}{B_1^2}\right) - \cos^2\beta\right]}{\cos^2\beta - B_1^2 K_I a \frac{1}{2}\sin 2\beta} \qquad (7)$$

may be obtained from the analysis of reference 3. When equation (7) is substituted into equation (6), β is set equal to $\theta - \alpha_o$ and $K_I a$ is defined by equation (3) with ϵ set equal to α_o. The variation of K_{II} with ϵ for a range of free-stream Mach numbers is presented in figure 5.

The corresponding formulas for the lift and pitching-moment coefficients expressed as rates of change with $\frac{\dot{\alpha}c}{2V_\infty}$ as $\dot{\alpha}$ approaches zero are as follows:

$$c_{l_{\dot{\alpha}}} = -\frac{2}{M_\infty}\left(-M_1\sqrt{\frac{p_1\rho_1}{p_\infty\rho_\infty}}\,K_{II} + \frac{M_2}{B_2^3}\sqrt{\frac{p_2\rho_2}{p_\infty\rho_\infty}}\right)_{\epsilon=\alpha_o}\cos\alpha_o$$

$$= c_{n_{\dot{\alpha}}}\cos\alpha_o \tag{8}$$

$$c_{m_{\dot{\alpha}}} = \left(\frac{\bar{\bar{x}}}{c} - \frac{2}{3}\right)c_{n_{\dot{\alpha}}} \tag{9}$$

The symbol $\bar{\bar{x}}$ represents the chordwise distance of the pitch-axis location from the leading edge of the wing as shown in figure 1(b). The positive direction of pitching moment is also indicated in this figure.

The variation of $\frac{c_{l_{\dot{\alpha}}}}{\cos\alpha_o}$ or the normal-force derivative with angle of attack α_o for free-stream Mach numbers M_∞ is shown in figure 6. Since $\frac{c_{l_{\dot{\alpha}}}}{\cos\alpha_o} = \frac{c_{m_{\dot{\alpha}}}}{\frac{\bar{\bar{x}}}{c} - \frac{2}{3}}$ for the flat-plate wing, the variations of $\frac{c_{l_{\dot{\alpha}}}}{\cos\alpha_o}$ in this figure can also be considered as variations of $\frac{c_{m_{\dot{\alpha}}}}{\frac{\bar{\bar{x}}}{c} - \frac{2}{3}}$ in which $\frac{\bar{\bar{x}}}{c}$ is equal to ξ. Some illustrative variations of $c_{l_{\dot{\alpha}}}$ with α_o and M_∞ are presented in figures 7 and 8, respectively. Some illustrative variations of $c_{m_{\dot{\alpha}}}$ with α_o and M_∞ for two pitch-axis locations, $\xi = 0.25$ and 0.50, are presented in figures 9 and 10, respectively.

Wedge section.- The pressure-difference coefficient, lift, and pitching-moment coefficient for the wing having a wedge airfoil section performing a plunging motion, that is, a motion with constant vertical acceleration, are determined in essentially the same way as that described for the wedge section at a perturbed angle of attack. The pressure-difference coefficients are

$$\Delta C_p^{\dot{\alpha}} = -\frac{\dot{\alpha}c}{2V_\infty}\frac{4}{M_\infty}\left[\left(-M_1\sqrt{\frac{p_1\rho_1}{p_\infty\rho_\infty}}\,K_{II}\right)_{\epsilon=\epsilon_l} + \left(\frac{M_2}{B_2^3}\sqrt{\frac{p_2\rho_2}{p_\infty\rho_\infty}}\right)_{\epsilon=\epsilon_u}\right] \qquad (\alpha_o > |\delta|) \tag{10a}$$

$$\Delta C_p^{\dot{\alpha}} = -\frac{\dot{\alpha}c}{2V_\infty}\frac{4}{M_\infty}\left[\left(-M_1\sqrt{\frac{p_1\rho_1}{p_\infty\rho_\infty}}\,K_{II}\right)_{\epsilon=\epsilon_l} + \left(-M_1\sqrt{\frac{p_1\rho_1}{p_\infty\rho_\infty}}\,K_{II}\right)_{\epsilon=-\epsilon_u}\right] \qquad (\alpha_o < |\delta|) \tag{10b}$$

The corresponding lift and pitching-moment derivatives are

$$c_{l_{\dot{\alpha}}} = c_{n_{\dot{\alpha},l}} \cos\left(\alpha_o + |\delta|\right) - c_{n_{\dot{\alpha},u}} \cos\left(\alpha_o - |\delta|\right) \qquad (\alpha_o > |\delta|) \qquad (11a)$$

$$c_{l_{\dot{\alpha}}} = c_{n_{\dot{\alpha},l}} \cos(\alpha_o + |\delta|) - c_{n_{\dot{\alpha},u}} \cos(|\delta| - \alpha_o) \qquad (\alpha_o < |\delta|) \qquad (11b)$$

and

$$c_{m_{\dot{\alpha}}} = \left(\xi \cos |\delta| - \frac{2}{3 \cos |\delta|}\right)\left(c_{n_{\dot{\alpha},l}} - c_{n_{\dot{\alpha},u}}\right) \qquad (12)$$

The quantities $c_{n_{\dot{\alpha},l}}$ and $c_{n_{\dot{\alpha},u}}$ are the normal-force derivatives of the lower and upper surfaces, respectively, of the wing and are equal to

$$c_{n_{\dot{\alpha},l}} = 2\left(\frac{M_1}{M_\infty}\sqrt{\frac{p_1\rho_1}{p_\infty\rho_\infty}}\, K_{II}\right)_{\epsilon=\epsilon_l}$$

$$c_{n_{\dot{\alpha},u}} = 2\left(\frac{M_2}{M_\infty B_2^3}\sqrt{\frac{p_2\rho_2}{p_\infty\rho_\infty}}\right)_{\epsilon=\epsilon_u} \qquad (\alpha_o > |\delta|)$$

$$c_{n_{\dot{\alpha},u}} = -2\left(\frac{M_1}{M_\infty}\sqrt{\frac{p_1\rho_1}{p_\infty\rho_\infty}}\, K_{II}\right)_{\epsilon=-\epsilon_u} \qquad (\alpha_o < |\delta|)$$

For zero angle of attack, $c_{n_{\dot{\alpha},l}} = -c_{n_{\dot{\alpha},u}}$ and equations (11b) and (12) may be written

$$\left(c_{l_{\dot{\alpha}}}\right)_{\alpha_o=0} = \left(4\,\frac{M_1}{M_\infty}\sqrt{\frac{p_1\rho_1}{p_\infty\rho_\infty}}\, K_{II}\right)_{\epsilon=\epsilon_l} \cos |\delta|$$

$$\left(c_{m_{\dot{\alpha}}}\right)_{\alpha_o=0} = \left(\xi \cos |\delta| - \frac{2}{3 \cos |\delta|}\right)\frac{\left(c_{l_{\dot{\alpha}}}\right)_{\alpha_o=0}}{\cos |\delta|}$$

The effect of wedge thickness on the $c_{l_{\dot{\alpha}}}$ variation with free-stream Mach number is presented in figure 11 for the wing at zero angle

of attack. Increasing the wedge angle or thickness increases the negative value of this derivative at a given free-stream Mach number. The effect of wedge thickness on the variation of the $c_{m_{\dot{\alpha}}}$ derivative with free-stream Mach number for various positions of the pitch axis is presented in figure 12 for the wing at zero angle of attack. Figure 13 presents some illustrative variations of this derivative with wedge thickness for different free-stream Mach numbers at zero angle of attack. Figure 14 is an illustration of the variation of $c_{m_{\dot{\alpha}}}$ with angle of attack for two thickness ratios and a range of Mach numbers. It should be emphasized that the validity of these derivatives for the higher angles of attack considered in these figures is questionable primarily because of the effect of viscous separation which probably restricts the usefulness of the results to a much smaller range of angle of attack. In addition, it should be pointed out that it is realized that the 14-percent-thick airfoil considered in figures 11 to 14 and in some successive figures is an example of extreme thickness; however, the variations of the derivatives for this thickness are presented in order to indicate a relative effect of thickness over a wide range of the thickness parameter.

Forces and Moments Produced by Slow Rotary Oscillations

For low-frequency oscillations of the wing, it has been demonstrated (see section entitled "Preliminary Remarks") that the oscillatory forces and moments may be approximated by the linear sum of these quantities for constant vertical acceleration and steady pitching motion. On this basis, the oscillatory lift and pitching moment in derivative form appropriate to stability studies may be expressed as $c_{l_q} + c_{l_{\dot{\alpha}}}$ and $c_{m_q} + c_{m_{\dot{\alpha}}}$, respectively.

The aerodynamic surface pressures and the force and moment coefficients due to pitching have been derived in reference 4; therefore, in this paper it is necessary to make use of only these results and the corresponding results for the constant vertical acceleration presented previously in order to determine the first-order oscillatory coefficients.

Flat-plate section.- The pressure difference in coefficient form is given by

$$\Delta C_p = \Delta C_p{}^{q} + \Delta C_p{}^{\dot{\alpha}}$$

where, from reference 4,

$$\Delta C_p{}^q = 4\,\frac{qc}{2V_\infty}\left[\frac{M_1}{M_\infty}\sqrt{\frac{p_1\rho_1}{p_\infty\rho_\infty}}\left(\frac{m - K_I a}{1 - K_I a B_1{}^2 m}\right)\frac{x}{c} + K_I a\xi + \right.$$

$$\left.\frac{M_2}{B_2 M_\infty}\sqrt{\frac{p_2\rho_2}{p_\infty\rho_\infty}}\left(\frac{x}{c} - \xi\right)\right]_{\epsilon=\alpha_o} \tag{13}$$

From equations (6) and (13) expressions for the lift and pitching-moment derivatives are given, respectively, by

$$c_{l_q} + c_{l_{\dot\alpha}} = \left[4\,\frac{M_1}{M_\infty}\sqrt{\frac{p_1\rho_1}{p_\infty\rho_\infty}}\left(K_{III} + K_I a\xi\right)\cos\alpha_o + \right.$$

$$\left. 4\,\frac{M_2}{B_2 M_\infty}\sqrt{\frac{p_2\rho_2}{p_\infty\rho_\infty}}\left(\frac{1}{2} - \xi - \frac{1}{2B_2{}^2}\right)\cos\alpha_o\right]_{\epsilon=\alpha_o} \tag{14}$$

and

$$c_{m_q} + c_{m_{\dot\alpha}} = \frac{\left(c_{l_q} + c_{l_{\dot\alpha}}\right)_{\xi=0}}{\cos\alpha_o}\left(\xi - \frac{2}{3}\right) + \left[-4K_I a\xi\left(\frac{1}{2} - \xi\right) + \right.$$

$$\left.\frac{4}{B_2}\,\frac{M_2}{M_\infty}\sqrt{\frac{p_2\rho_2}{p_\infty\rho_\infty}}\,\xi\left(\frac{1}{2} - \xi\right)\right]_{\epsilon=\alpha_o} \tag{15}$$

where $\left(c_{l_q} + c_{l_{\dot\alpha}}\right)_{\xi=0}$ is the value of the lift derivative for the pitch axis located at the leading edge ($\xi = 0$). The parameter K_{III} appearing in equation (14) is

$$K_{III} = \frac{m - K_I a}{1 - K_I a B_1{}^2 m} + K_{II} \tag{16}$$

The variation of this parameter with free-stream Mach number and angle of attack is presented in figure 15.

The variation of $\frac{c_{l_q} + c_{l_{\dot{\alpha}}}}{\cos \alpha_o}$ or the normal-force derivative with angle of attack for free-stream Mach numbers are presented in figure 16 for the pitch axis located at the leading edge ($\xi = 0$). Illustrative variations of the lift derivative $c_{l_q} + c_{l_{\dot{\alpha}}}$ and the pitching-moment derivative $c_{m_q} + c_{m_{\dot{\alpha}}}$ with angle of attack and with Mach number for different locations of the pitch axis are given in figures 17 to 20. In order that the effect of thickness might be made readily apparent, Mach number and angle-of-attack variations of $c_{m_q} + c_{m_{\dot{\alpha}}}$ for a 7-percent-thick wedge section have been prepared as figure 21. These same variations for the flat-plate wing are presented in figure 20. More extensive variations of the various aerodynamic coefficients for the wedge section are introduced subsequently.

Wedge section.- The pressure-difference coefficient, lift, and pitching-moment coefficient for the wedge section performing a low-frequency oscillatory motion are determined by the same procedure used in obtaining these quantities for the wedge executing a constant vertical acceleration. The pressure-difference coefficient is

$$\Delta C_p = \Delta C_p{}^q + \Delta C_p{}^{\dot{\alpha}}$$

From reference 4, $\Delta C_p{}^q$ may be expressed as

$$\Delta C_p{}^q = 4 \frac{qc}{2V_\infty} \left\{ \left(\frac{M_1}{M_\infty} \sqrt{\frac{p_1 \rho_1}{p_\infty \rho_\infty}} K_{III} \frac{x}{c} + K_I a \xi \cos |\delta| \right)_{\epsilon=\epsilon_l} + \left[\frac{M_2}{B_2 M_\infty} \sqrt{\frac{p_2 \rho_2}{p_\infty \rho_\infty}} \left(\frac{x}{c} - \xi \cos |\delta| \right) \right]_{\epsilon=\epsilon_u} \right\} \qquad (\alpha_o > |\delta|) \qquad (17a)$$

and

$$\Delta C_p{}^q = 4 \frac{qc}{2V_\infty} \left[\left(\frac{M_1}{M_\infty} \sqrt{\frac{p_1 \rho_1}{p_\infty \rho_\infty}} K_{III} \frac{x}{c} + K_I a \xi \cos |\delta| \right)_{\epsilon=\epsilon_l} + \left(\frac{M_1}{M_\infty} \sqrt{\frac{p_1 \rho_1}{p_\infty \rho_\infty}} K_{III} \frac{x}{c} + K_I a \xi \cos |\delta| \right)_{\epsilon=-\epsilon_u} \right] \qquad (\alpha < |\delta|) \qquad (17b)$$

This expression for $\Delta C_p{}^q$ of the wedge airfoil section is not exact but is an excellent approximation of the correct linearized expression for pressure difference due to pitching. The approximation arises from the use for the wedge airfoil section of the pressure expressions for the flat-plate airfoil section, that is, pitching about an axis located in the plane of the plate. For the wedge section, however, the pitching axis is not located in either plane of the wedge surface but is located in the chord plane of symmetry. (See fig. 1.) The prescribed velocity distribution along the wedge surfaces, therefore, is identical to the prescribed velocity distribution along the surface of a flat plate pitching about an axis that is displaced from the plane of the plate and not about an axis located in the plane of the plate. This displacement of the pitch axis produces small changes in the magnitude and inclination of the surface velocity distribution and, hence, in the pressure distribution that is not accounted for by the application of the flat-plate pressure expressions. For semiapex angles of the wedge that are 10° or less, the effect of the pitching-axis displacement is negligible and equations (17) as stated previously are an excellent approximation to the exact linearized pressure. For larger semiapex angles (say 15°), equations (17) are still adequate for theoretical estimates of pressure due to the pitching motion. From equations (10) for $\Delta C_p{}^{\dot{\alpha}}$ and equations (17), the corresponding expressions for the lift and pitching-moment derivatives, respectively, are as follows:

$$c_{l_q} + c_{l_{\dot{\alpha}}} = \left\{\frac{4}{M_\infty}\left[M_1\sqrt{\frac{p_1\rho_1}{p_\infty\rho_\infty}}\left(K_{III} + K_I a\xi\cos|\delta|\right)\right]\cos\left(\alpha_o + |\delta|\right)\right\}_{\epsilon=\epsilon_l} + \left\{\frac{4}{M_\infty}\left[\frac{M_2}{B_2}\sqrt{\frac{p_2\rho_2}{p_\infty\rho_\infty}}\left(\frac{1}{2} - \xi\cos|\delta| - \frac{1}{2B_2{}^2}\right)\right]\cos\left(\alpha_o - |\delta|\right)\right\}_{\epsilon=\epsilon_u}$$

$$(\alpha_o > |\delta|) \qquad (18a)$$

$$c_{l_q} + c_{l_{\dot{\alpha}}} = \left\{\frac{4}{M_\infty}\left[M_1\sqrt{\frac{p_1\rho_1}{p_\infty\rho_\infty}}\left(K_{III} + K_I a\xi\cos|\delta|\right)\right]\cos\left(\alpha_o + |\delta|\right)\right\}_{\epsilon=\epsilon_l} + \left\{\frac{4}{M_\infty}\left[M_1\sqrt{\frac{p_1\rho_1}{p_\infty\rho_\infty}}\left(K_{III} + K_I a\xi\cos|\delta|\right)\right]\cos\left(|\delta| - \alpha_o\right)\right\}_{\epsilon=-\epsilon_u}$$

$$\left(\alpha_o < |\delta|\right) \qquad (18b)$$

and

$$c_{m_q} + c_{m_{\dot{\alpha}}} = \left[4 \frac{M_1}{M_\infty} \sqrt{\frac{p_1 \rho_1}{p_\infty \rho_\infty}} K_{III} \left(\xi \cos |\delta| - \frac{2}{3 \cos |\delta|} \right) - 4 K_I a \xi \cos |\delta| \left(\frac{1}{2} - \xi \cos |\delta| \right) \right]_{\epsilon=\epsilon_l} +$$

$$\left[4 \frac{M_2}{M_\infty B_2} \sqrt{\frac{p_2 \rho_2}{p_\infty \rho_\infty}} K_{III} \left(\frac{1}{2} - \frac{1}{2 B_2^2} \right) \left(\xi \cos |\delta| - \frac{2}{3 \cos |\delta|} \right) - 4 \frac{M_2}{M_\infty B_2} \sqrt{\frac{p_2 \rho_2}{p_\infty \rho_\infty}} \xi \cos |\delta| \left(\frac{1}{2} - \xi \cos |\delta| \right) \right]_{\epsilon=\epsilon_u} \qquad (\alpha > |\delta|) \qquad (19a)$$

$$c_{m_q} + c_{m_{\dot{\alpha}}} = \left[4 \frac{M_1}{M_\infty} \sqrt{\frac{p_1 \rho_1}{p_\infty \rho_\infty}} K_{III} \left(\xi \cos |\delta| - \frac{2}{3 \cos |\delta|} \right) - 4 K_I a \xi \cos |\delta| \left(\frac{1}{2} - \xi \cos |\delta| \right) \right]_{\epsilon=\epsilon_l} +$$

$$\left[4 \frac{M_1}{M_\infty} \sqrt{\frac{p_1 \rho_1}{p_\infty \rho_\infty}} K_{III} \left(\xi \cos |\delta| - \frac{2}{3 \cos |\delta|} \right) - 4 K_I a \xi \cos |\delta| \left(\frac{1}{2} - \xi \cos |\delta| \right) \right]_{\epsilon=-\epsilon_u} \qquad (\alpha < |\delta|) \qquad (19b)$$

As indicated previously, the values of the derivatives at zero angle of attack are equal to twice the values of these quantities determined for the lower surface:

$$\left(c_{l_q} + c_{l_{\dot{\alpha}}} \right)_{\alpha=0} = 8 \frac{M_1}{M_\infty} \sqrt{\frac{p_1 \rho_1}{p_\infty \rho_\infty}} \left(K_{III} + K_I a \xi \cos |\delta| \right) \cos |\delta|$$

$$\left(c_{m_q} + c_{m_{\dot{\alpha}}}\right)_{\alpha=0} = \left(c_{n_q} + c_{n_{\dot{\alpha}}}\right)_{\substack{\alpha=0 \\ \xi=0}}\left(\xi \cos|\delta| - \frac{2}{3\cos|\delta|}\right) -$$

$$8K_I a\xi \cos|\delta|\left(\frac{1}{2} - \xi \cos|\delta|\right)$$

Illustrative variations of the effect of wedge thickness for zero angle of attack on the lift and pitching-moment derivatives are presented in figures 22 to 24. The effect of wedge thickness on the variation of $c_{m_q} + c_{m_{\dot{\alpha}}}$ with angle of attack for various Mach numbers is shown in figure 25. In this figure for the angle-of-attack range near zero, an increase in thickness tends to decrease the pitching-moment coefficient at the lowest Mach number but increases it at the higher Mach numbers. At high angles of attack $(\alpha_o > 20^\circ)$ and Mach numbers, increased thickness results in a decrease in damping at a given angle of attack.

An indication of the effect of angle of attack and thickness on the pitching-moment neutral-stability boundary $\left(c_{m_q} + c_{m_{\dot{\alpha}}} = 0\right)$ can be obtained from figures 26 and 27, respectively. Increasing angle of attack or increasing thickness tends to expand the range of Mach number and pitch-axis locations for which pitching instability occurs $\left(c_{m_q} + c_{m_{\dot{\alpha}}} > 0\right)$.

In reference 4 it is shown that a good approximation of c_{m_q}, the steady-state part of the pitching-moment coefficient, can be obtained by assuming that the effect of the shock on the perturbed flow can be neglected. In addition, it was assumed that the perturbed-flow components could be expressed as the derivatives of a potential function, based upon the unperturbed velocity V_1 of the shock flow along the lower surface of the airfoil. These same assumptions were used in reference 4 to calculate approximate values of $c_{m_{\dot{\alpha}}}$, the time-dependent part of the pitching-moment coefficient $c_{m_q} + c_{m_{\dot{\alpha}}}$. A comparison of this approximation of $c_{m_{\dot{\alpha}}}$ with the more rigorous estimates presented herein is given in figure 28. It is observed that the approximate derivative predicts the variation of the exact derivative with angle of attack for different Mach numbers, although the accuracy of the approximation may be objectionable for refined estimates of the pitching moment.

Possibly, a more accurate approximation to the linearized rotational-flow value of the pitching moment is the second-order solution developed by Van Dyke in reference 8 which is compared with the rotational-flow solution in reference 2. This comparison was for the neutral-stability boundary at zero angle of attack of a wedge with a 5° semiapex angle and

showed, for this wedge, excellent agreement between the second-order and rotational-flow solutions.

CONCLUDING REMARKS

Calculations have been made for the effect of angle of attack and wedge thickness on the aerodynamic coefficients of a wing performing a plunging motion and rotary oscillations at very low frequencies in two-dimensional flow. The results presented are for a range of angle of attack, wing thickness, and Mach number for which the flow behind the shock attached to the leading edge is everywhere supersonic, although the effect of viscous separation at the finite angles of attack restricts the validity of the results to a much smaller range of these parameters.

The results of the analysis and calculations show that for the flat-plate section and wedge section of finite thickness, increasing Mach number, for a fixed angle of attack of the wing, decreases the positive (destabilizing) values of the pitching-moment derivative $c_{m_q} + c_{m_{\dot{\alpha}}}$ and eventually causes the values of the derivative to become negative (stabilizing). For a fixed Mach number, increasing the angle of attack of the wing in the moderate and high angle-of-attack range decreases the negative value of the pitching-moment derivative. This effect becomes more predominant with increasing wedge thickness and rearward movements of the pitching-axis location.

The ranges of Mach number and pitch-axis location for which pitching instability occurs are increased with an increase in angle of attack and an increase in thickness.

Langley Aeronautical Laboratory,
National Advisory Committee for Aeronautics,
Langley Field, Va., May 28, 1957.

REFERENCES

1. Landahl, Marten, Mollo-Christensen, Erik L., and Ashley, Holt: Parametric Studies of Viscous and Nonviscous Unsteady Flows. OSR Tech. Rep. No. 55-13 (MIT Fluid Dynamics Res. Group Rep. No. 55-1, Contract No. AF18(600)-961), U. S. Air Force, Apr. 1955.

2. Van Dyke, Milton D.: On Supersonic Flow Past an Oscillating Wedge. Quarterly Appl. Math., vol. XI, no. 3, Oct. 1953, pp. 360-363.

3. Sewell, Geoffrey L.: A Theory of Uniform Supersonic Flow Past a Thin Oscillating Aerofoil at Appreciable Incidence to the Main Stream. Aero. Quarterly, vol. V, pt. 3, Sept. 1954, pp. 185-194.

4. Martin, John C., and Malvestuto, Frank S., Jr.: Aerodynamics of a Rectangular Wing of Infinite Aspect Ratio at High Angles of Attack and Supersonic Speeds. NACA TN 3421, 1955.

5. Carrier, G. F.: On the Stability of the Supersonic Flows Past a Wedge. Quarterly Appl. Math., vol. VI, no. 4, Jan. 1949, pp. 367-378.

6. Ames Research Staff: Equations, Tables, and Charts for Compressible Flow. NACA Rep. 1135, 1953. (Supersedes NACA TN 1428.)

7. Chu, Boa-Teh: On Weak Interaction of Strong Shock and Mach Waves Generated Downstream of the Shock. Jour. Aero. Sci., vol. 19, no. 7, July 1952, pp. 433-446.

8. Van Dyke, Milton D.: Supersonic Flow Past Oscillating Airfoils Including Nonlinear Thickness Effects. NACA Rep. 1183, 1954. (Supersedes NACA TN 2982.)

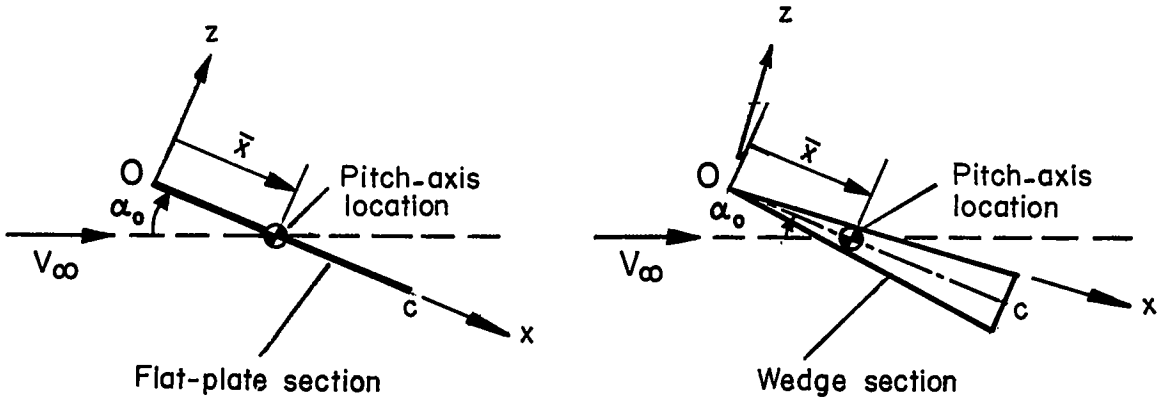

(a) Coordinate-axis system used in analysis. Expressions for surface pressures are presented relative to this system; for wedge section, the distance $\bar{x}$ is measured parallel to line of symmetry.

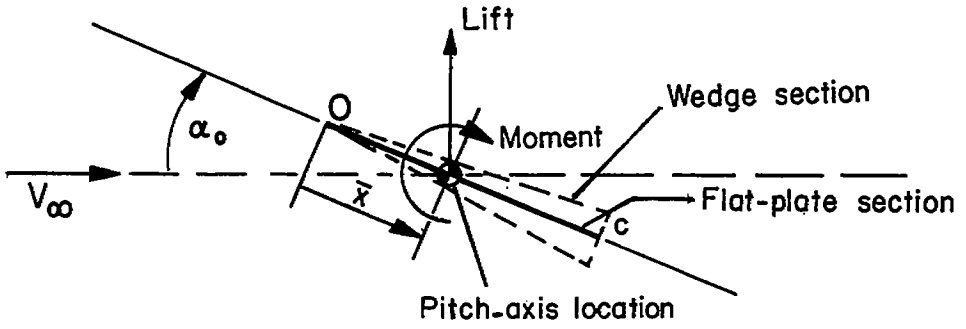

(b) Positive directions of lift and pitching moment for flat-plate and wedge sections.

Figure 1.- Airfoil sections and axes systems.

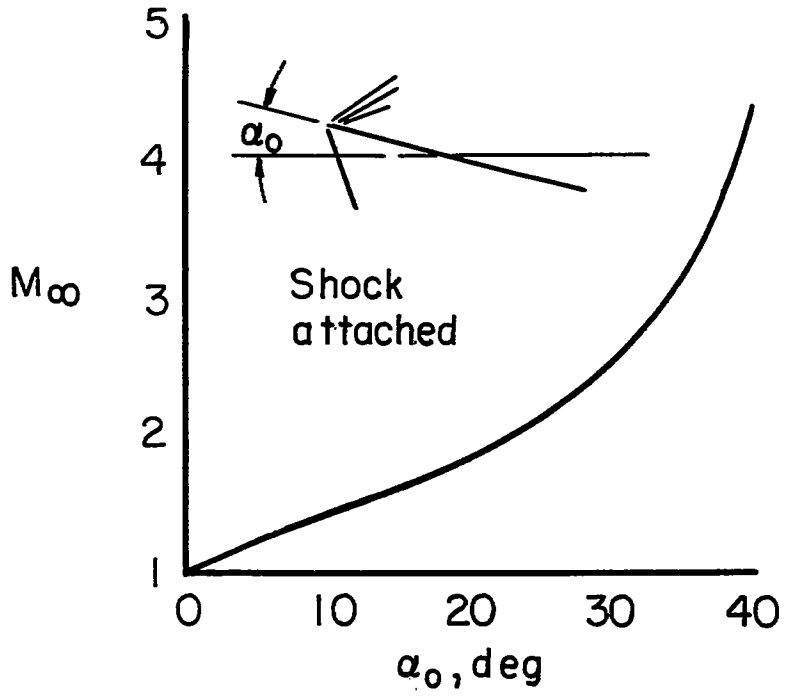

(a) Flat-plate section.

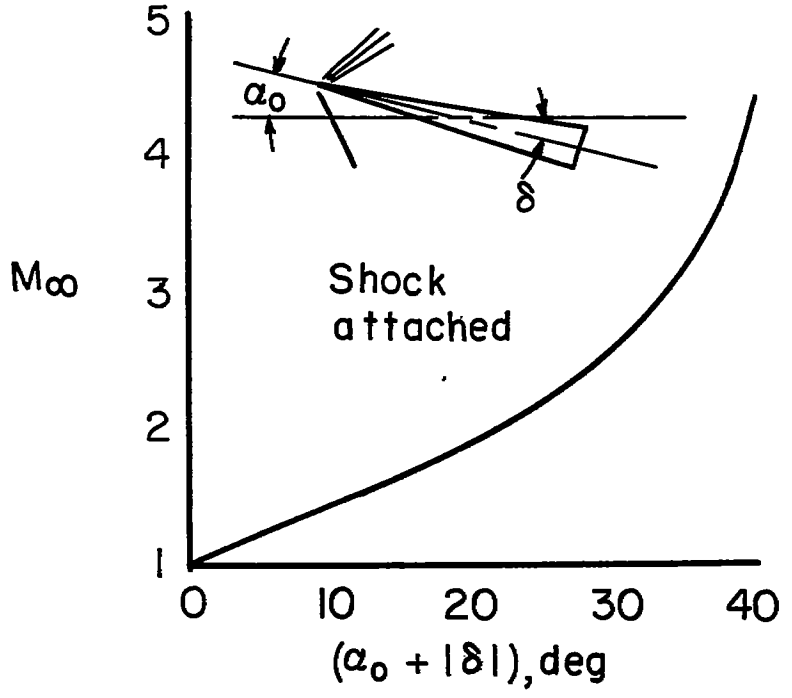

(b) Wedge section.

Figure 2.- Lower surface angle limitation for attached shock.

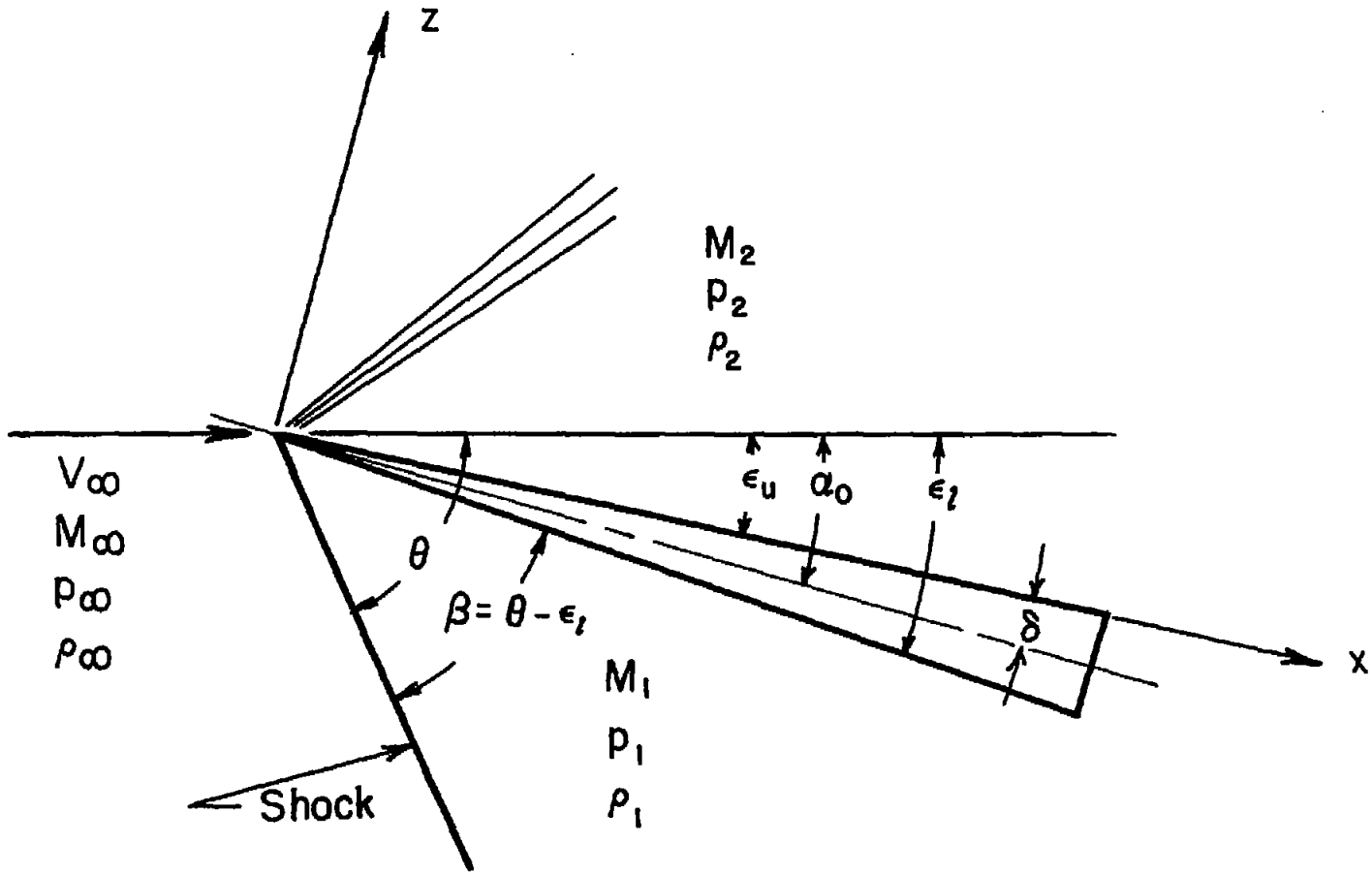

Figure 3.- Illustration of angles and flow parameters.

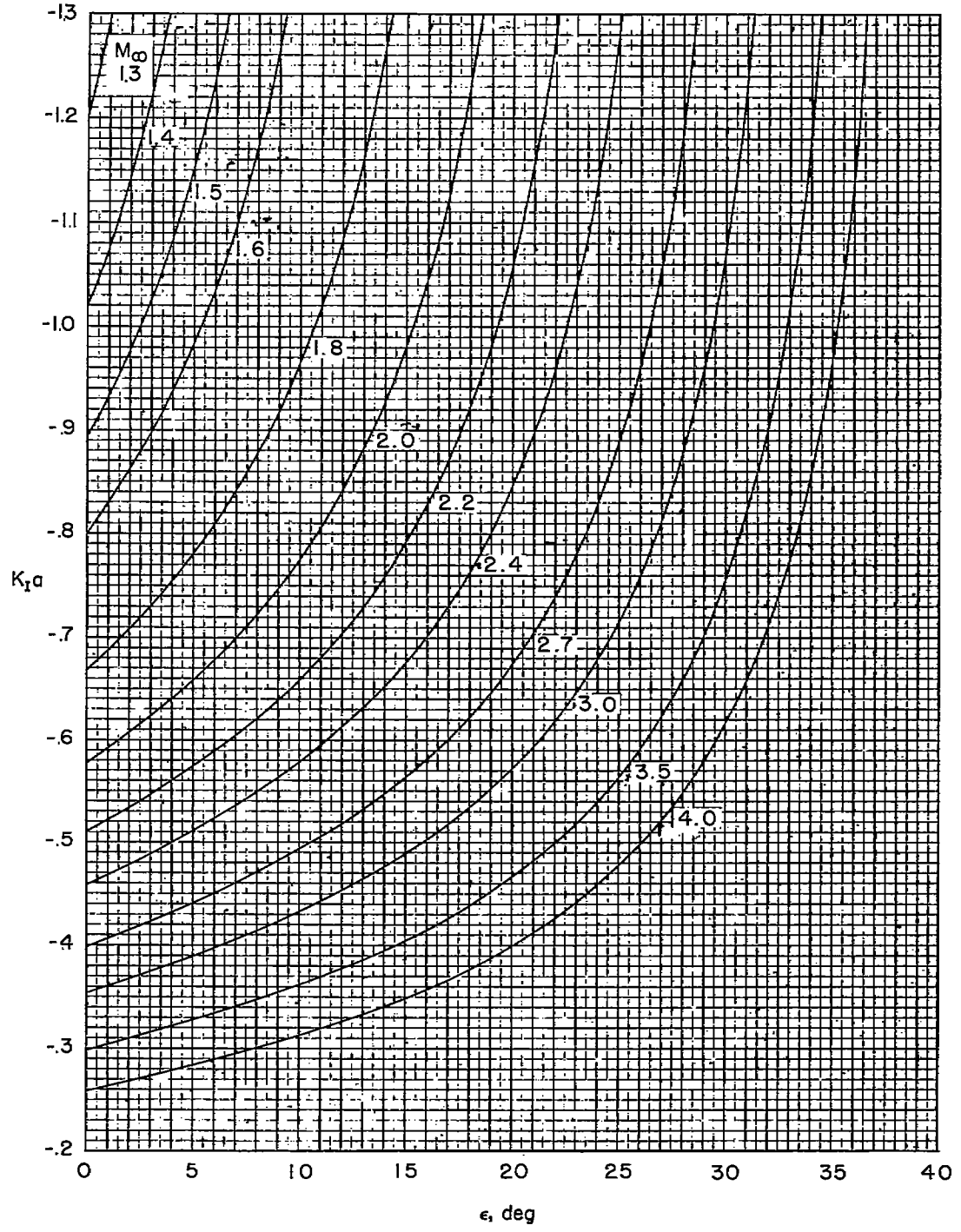

Figure 4.- Variation of $K_I a$ with ϵ for various free-stream Mach numbers.

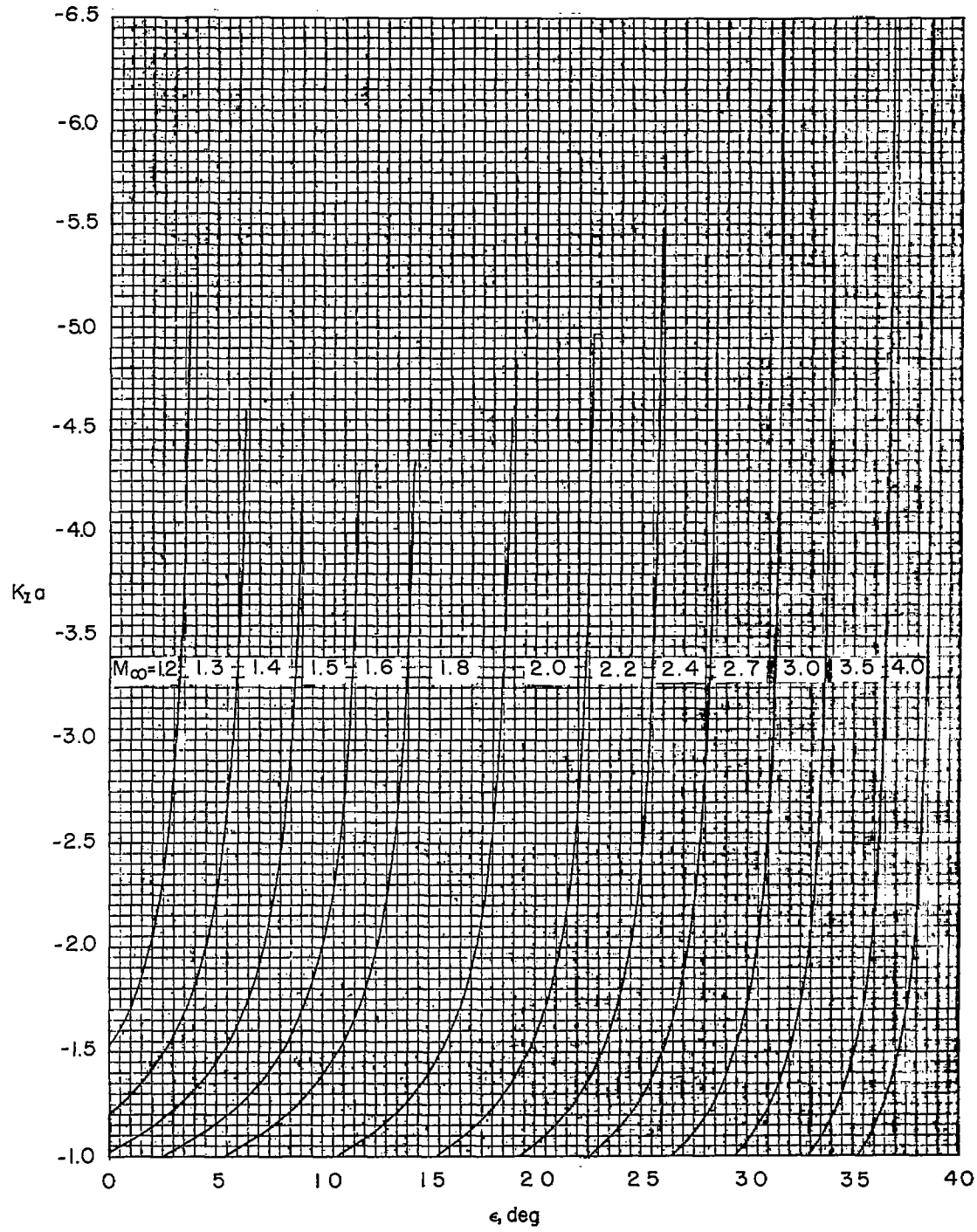

Figure 4.- Concluded.

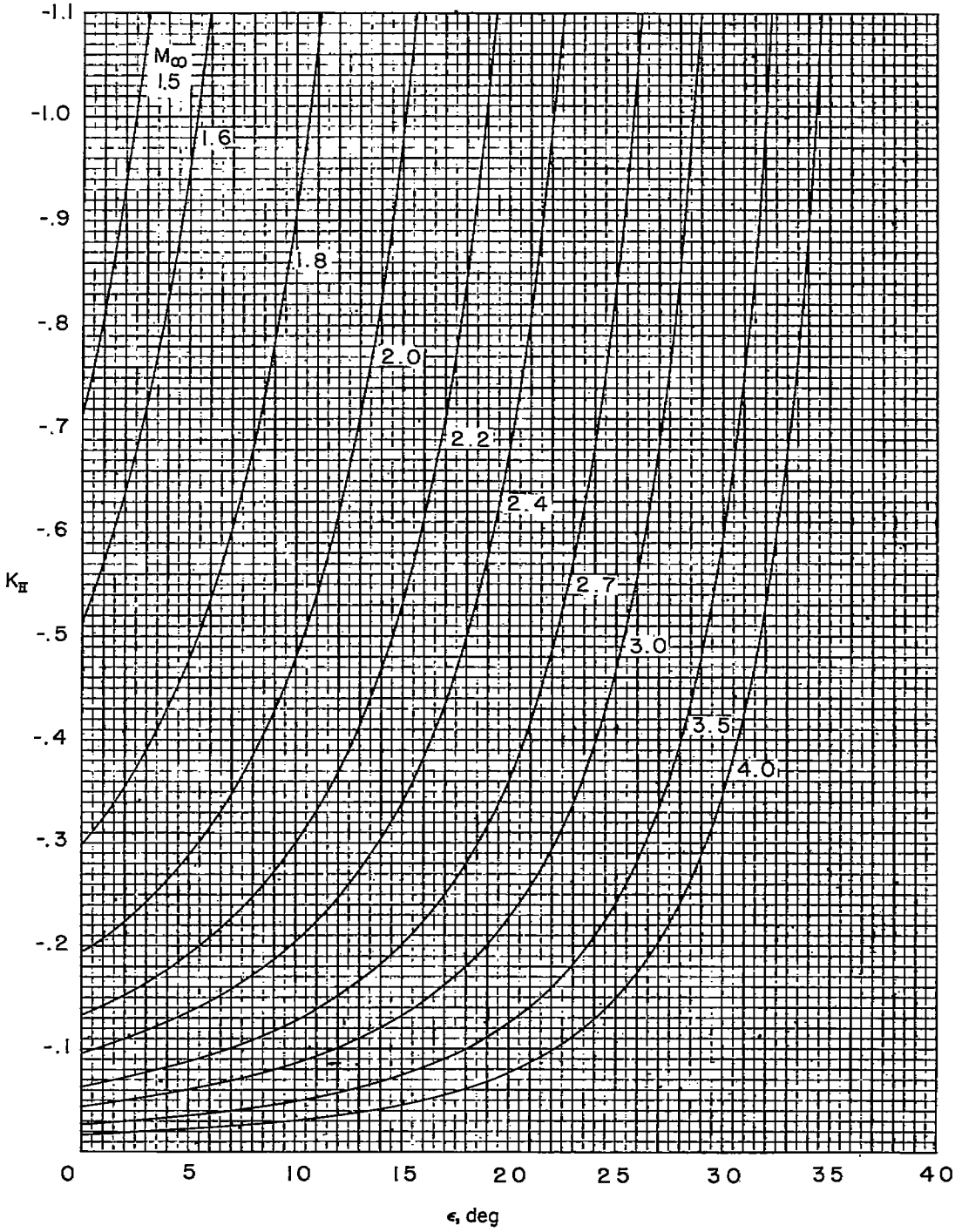

Figure 5.- Variation of K_{II} with ϵ for a range of free-stream Mach numbers.

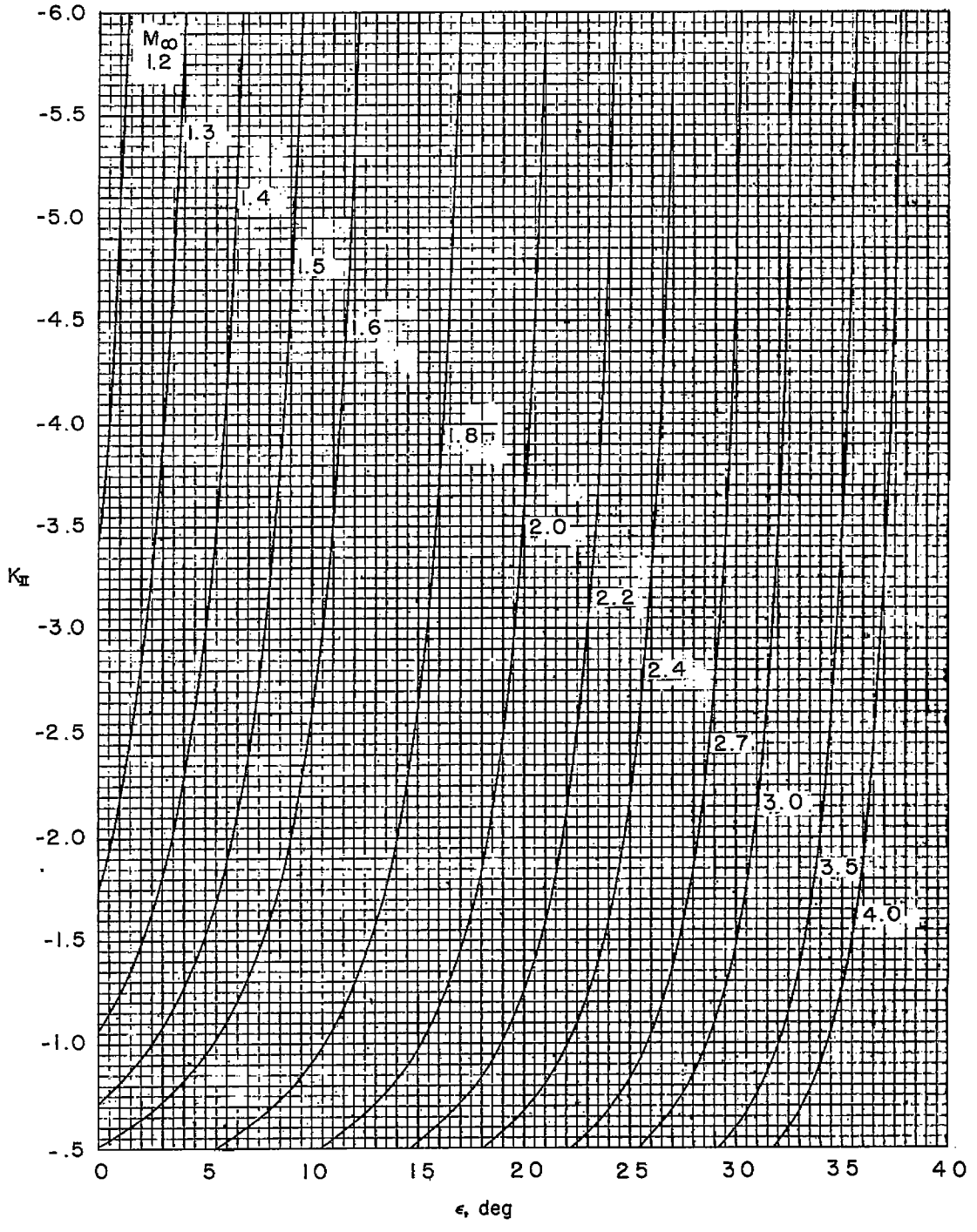

Figure 5.- Concluded.

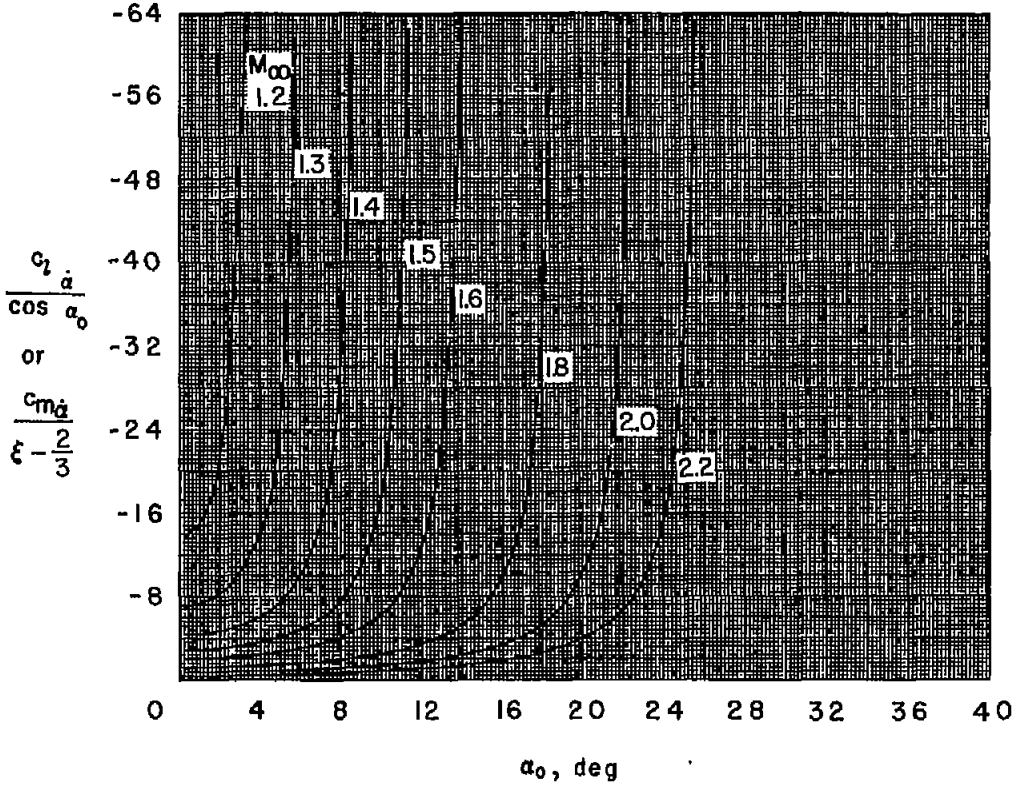

Figure 6.- Variation of $\frac{c_{l_{\dot{\alpha}}}}{\cos \alpha_o}$ $\left(\text{or } \frac{c_{m_{\dot{\alpha}}}}{\xi - 2/3}\right)$ with angle of attack for various free-stream Mach numbers.

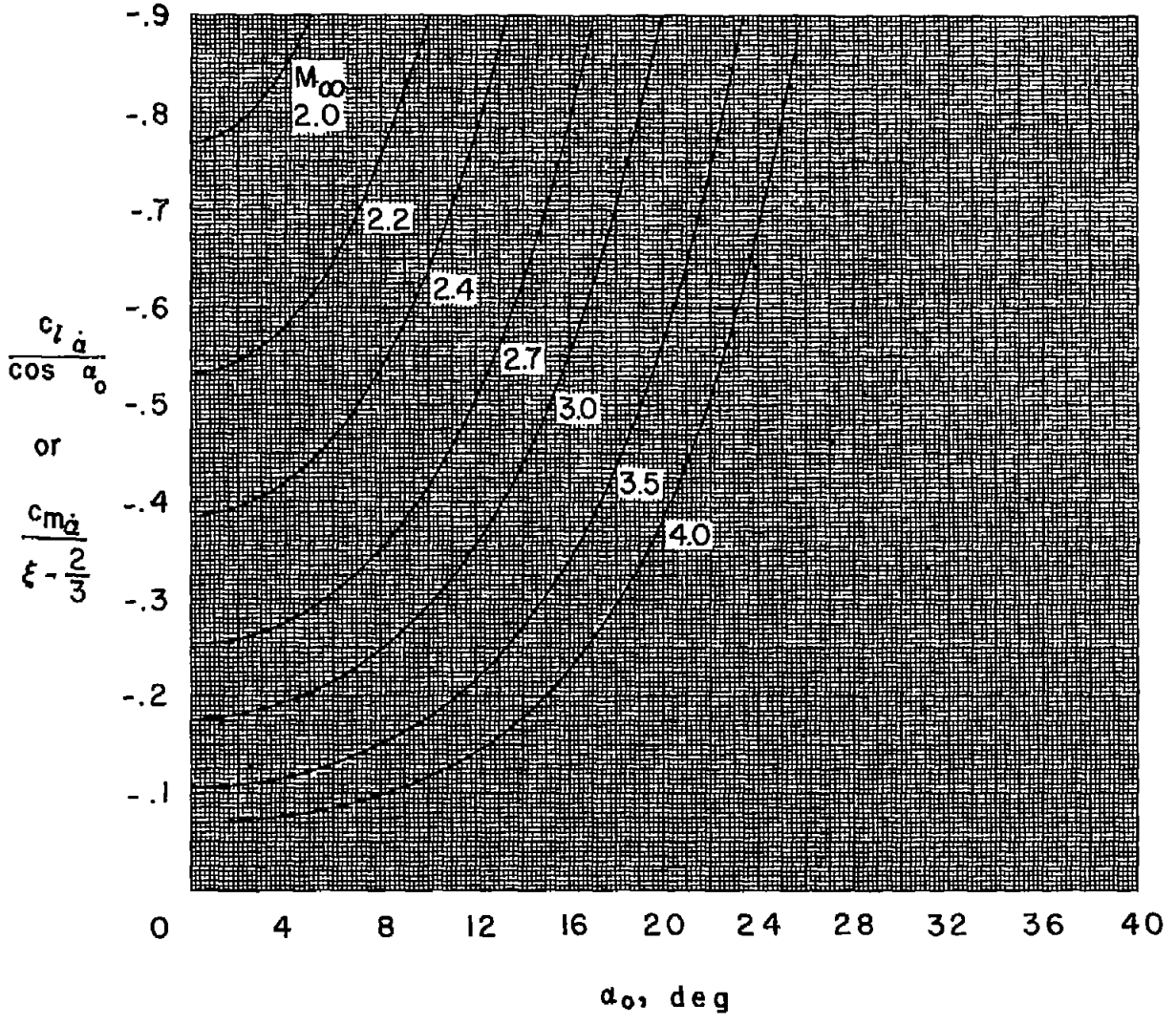

Figure 6.- Continued.

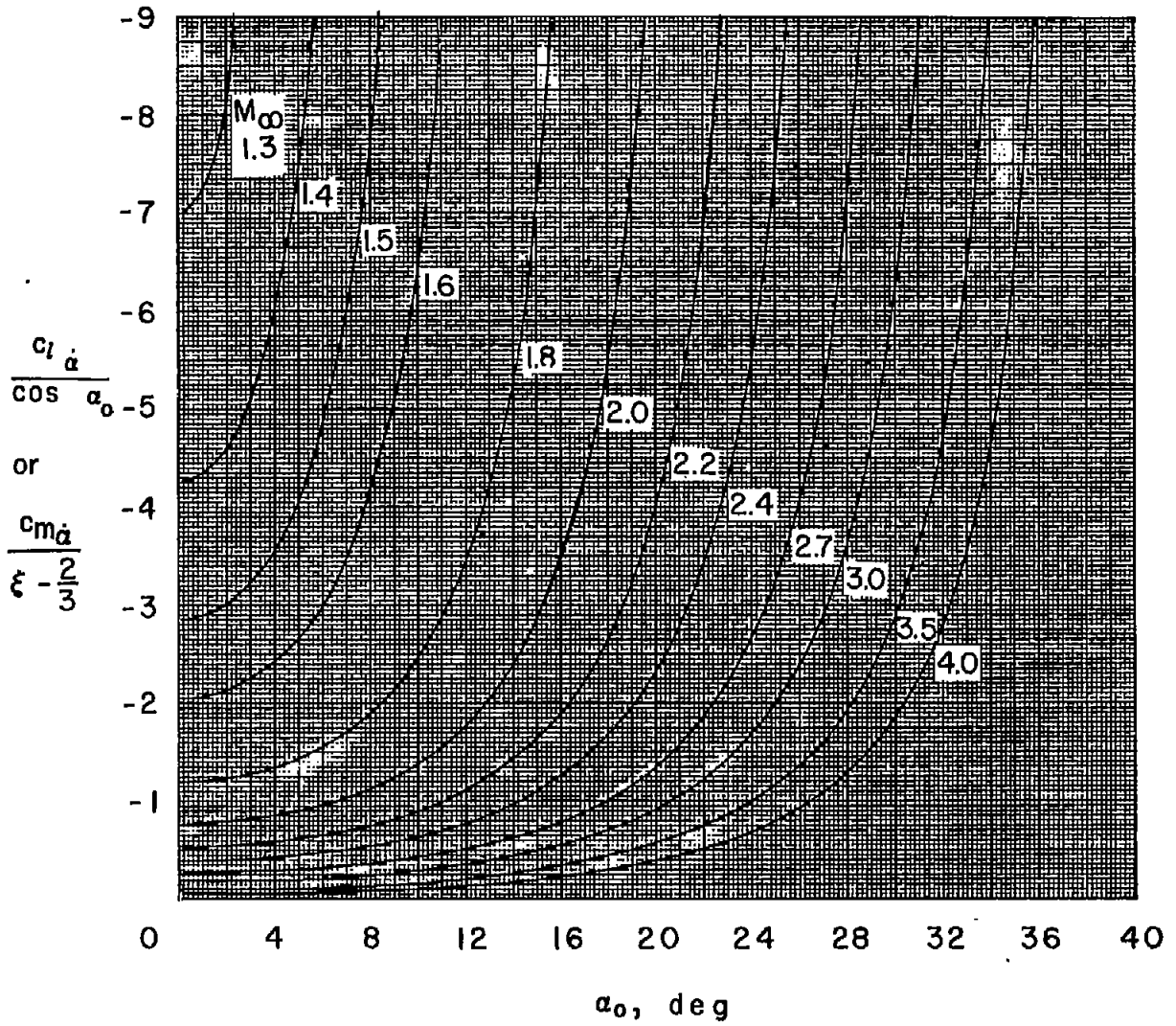

Figure 6.- Concluded.

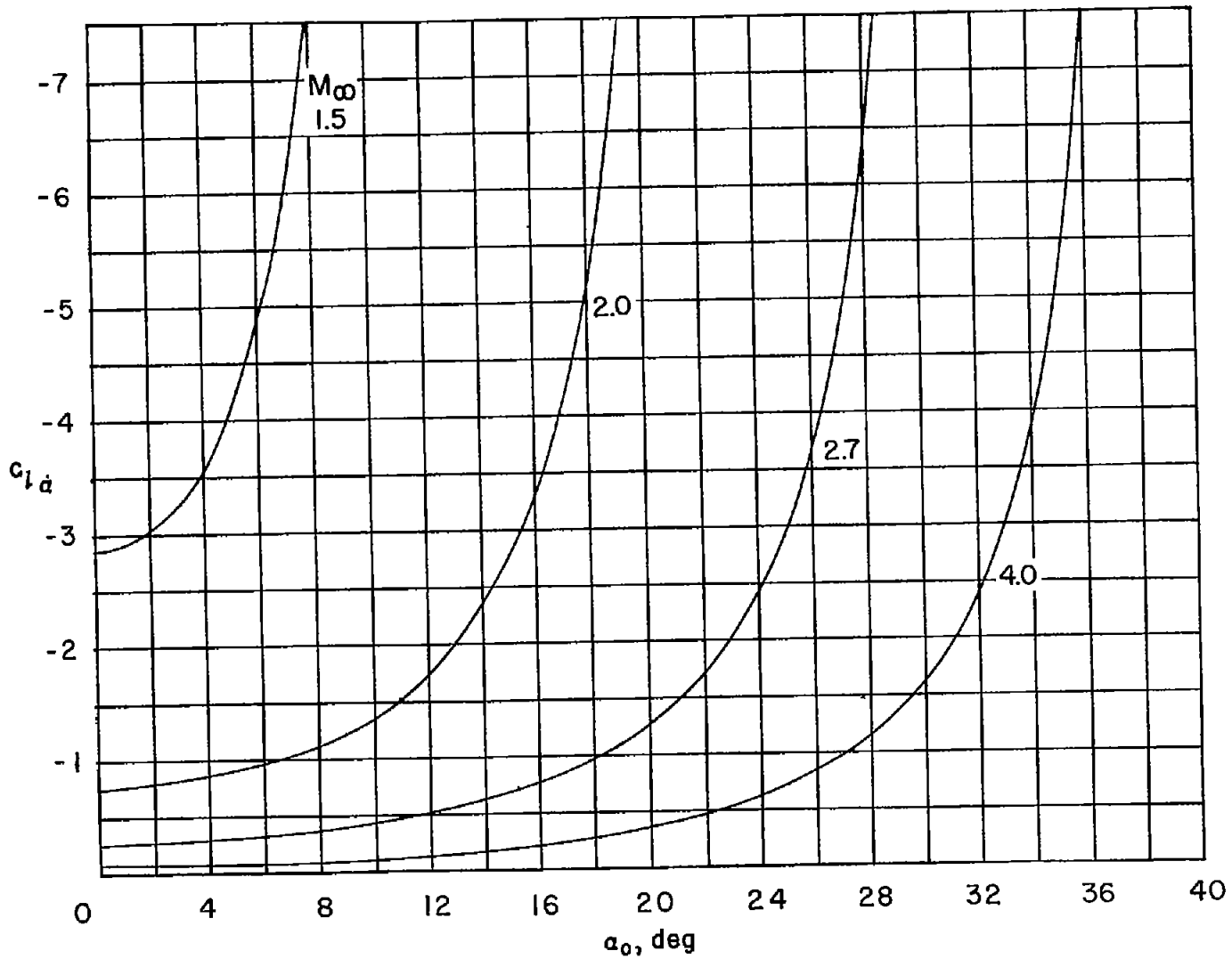

Figure 7.- Illustrative variation of $c_{l_{\dot{\alpha}}}$ with angle of attack for various free-stream Mach numbers.

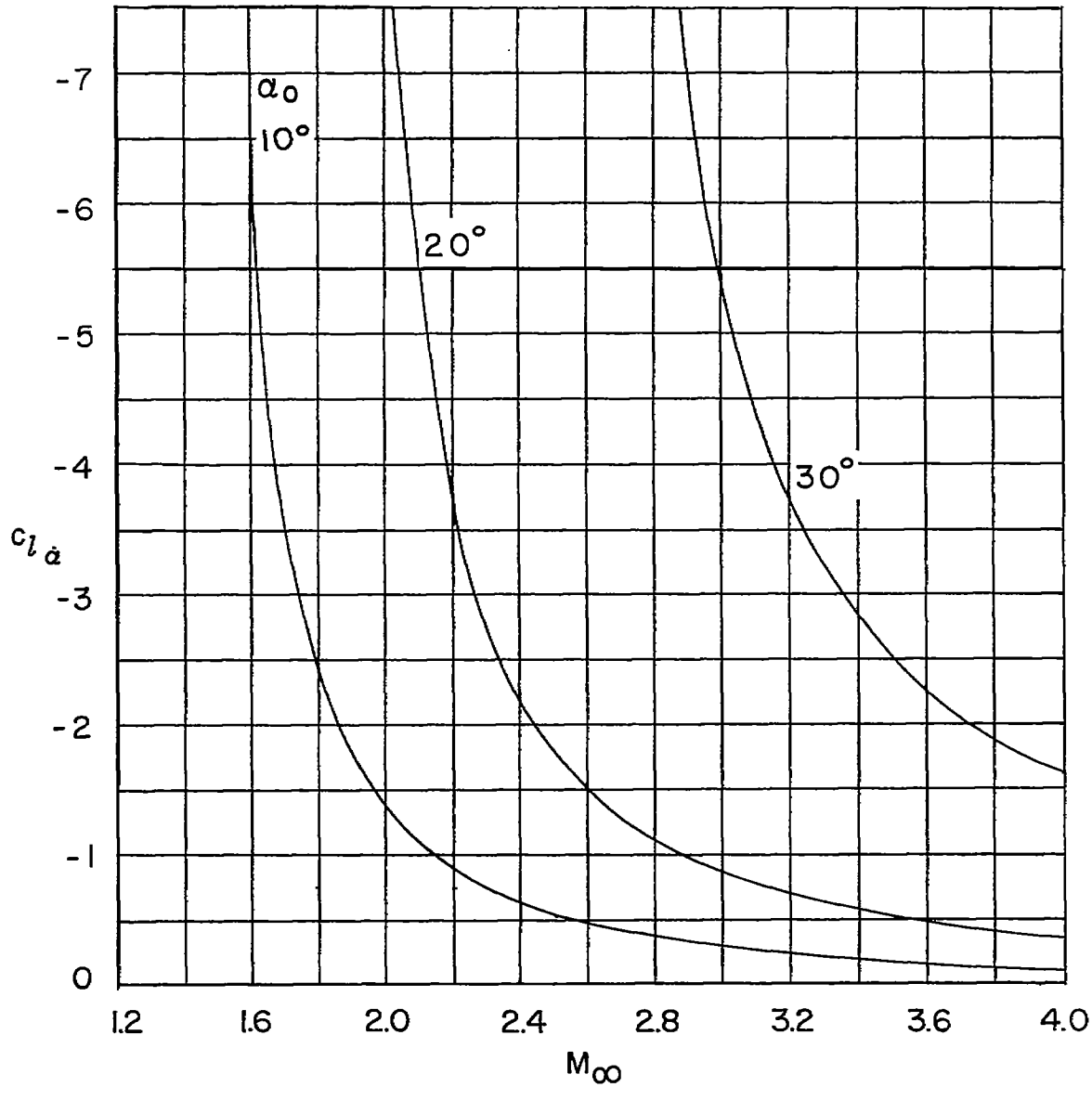

Figure 8.- Illustrative variation of $c_{l_{\dot{\alpha}}}$ with Mach number for various angles of attack.

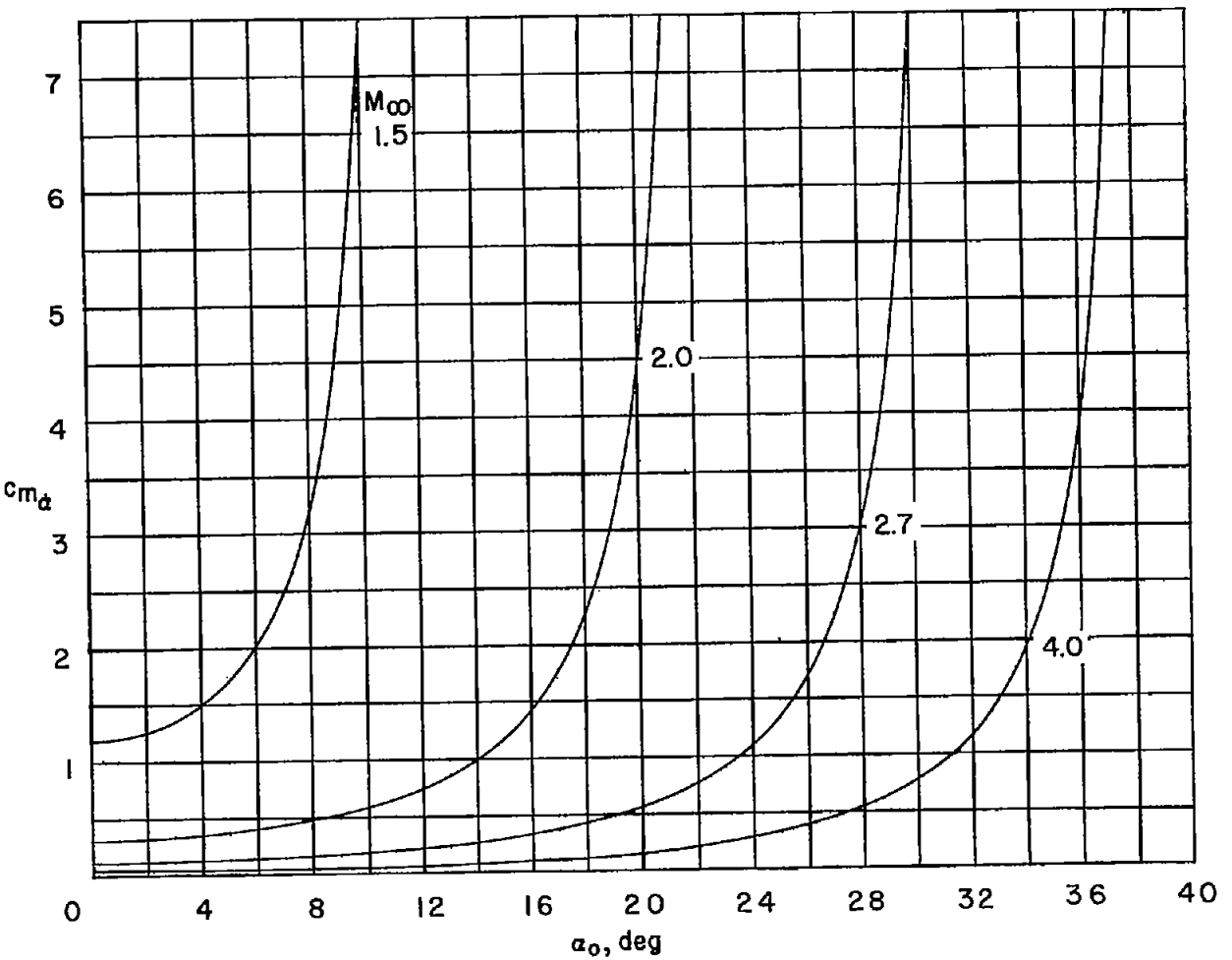

(a) $\xi = 0.25$.

Figure 9.- Illustrative variation of c_{m_α} with angle of attack for various free-stream Mach numbers.

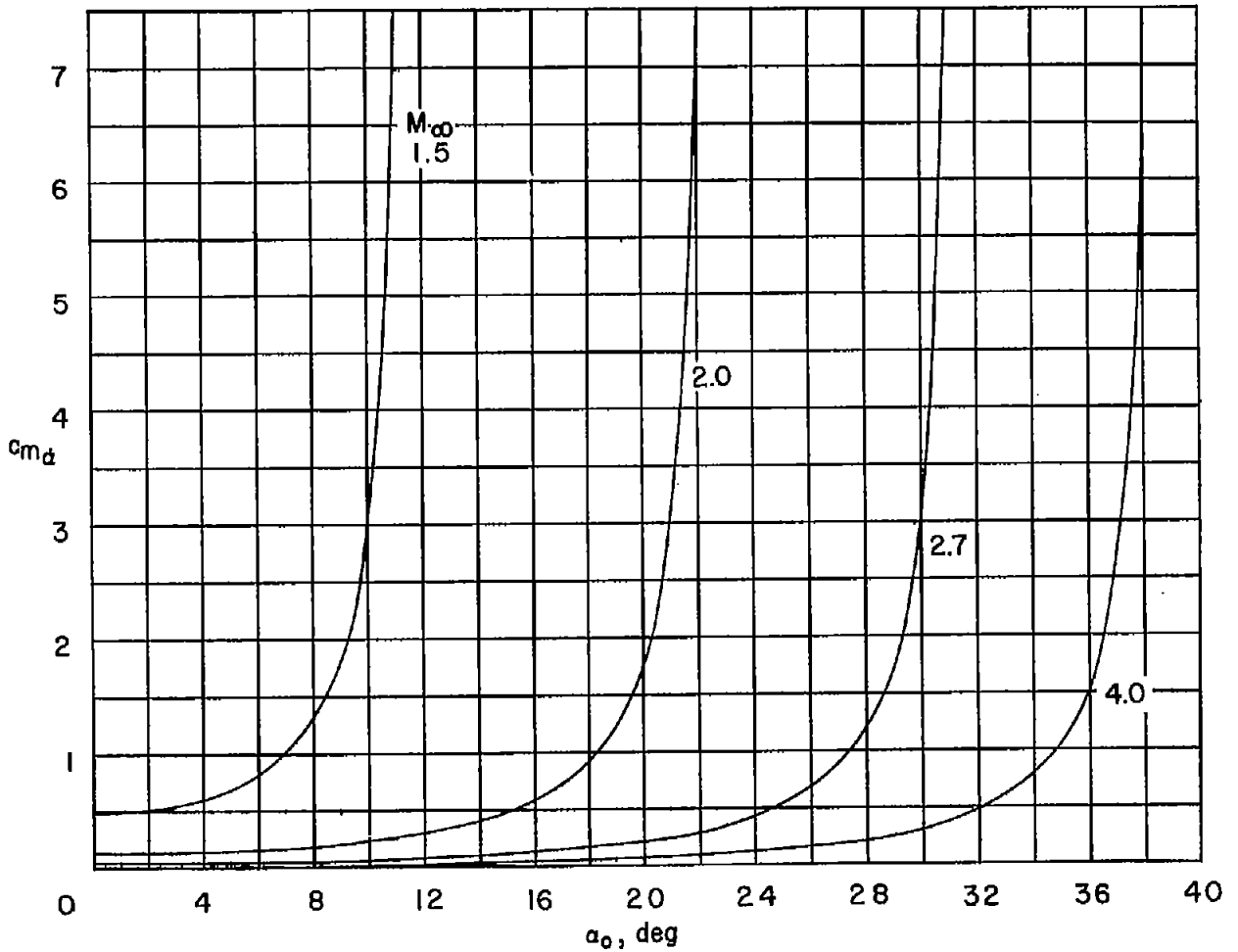

(b) $\xi = 0.50$.

Figure 9.- Concluded.

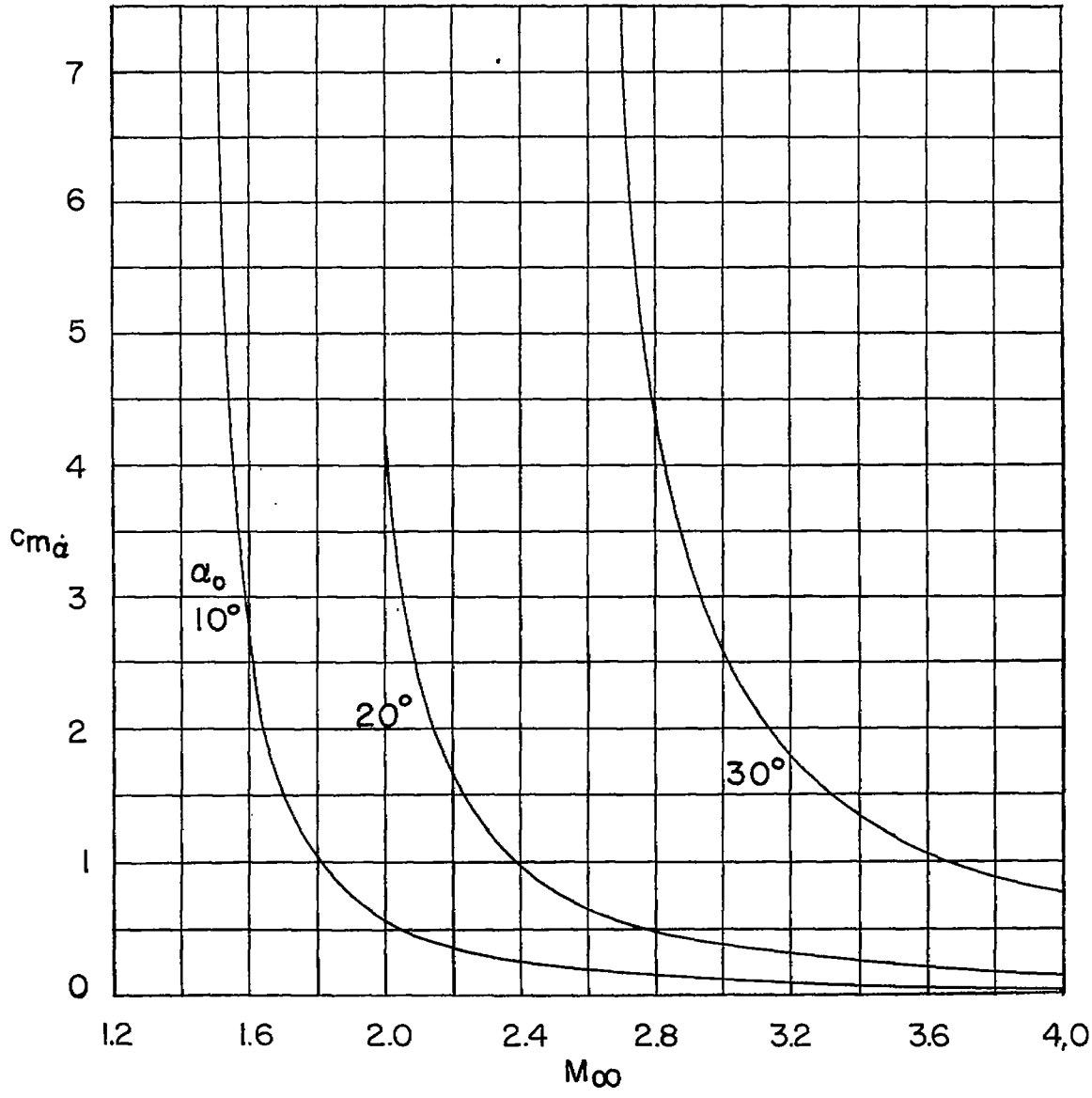

(a) $\xi = 0.25$.

Figure 10.- Illustrative variation of $c_{m_{\dot{\alpha}}}$ with free-stream Mach number for various angles of attack.

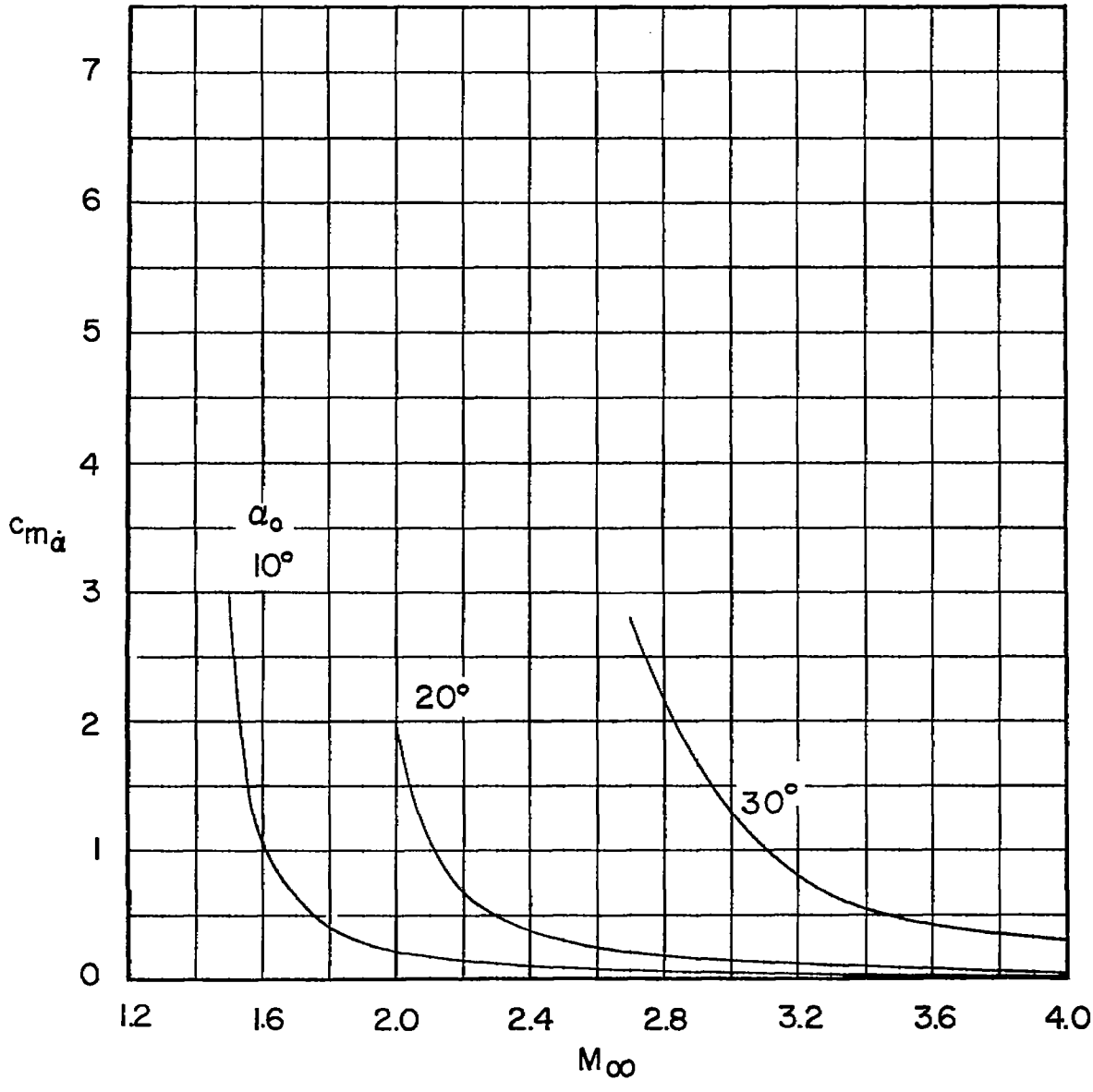

(b) $\xi = 0.50$.

Figure 10.- Concluded.

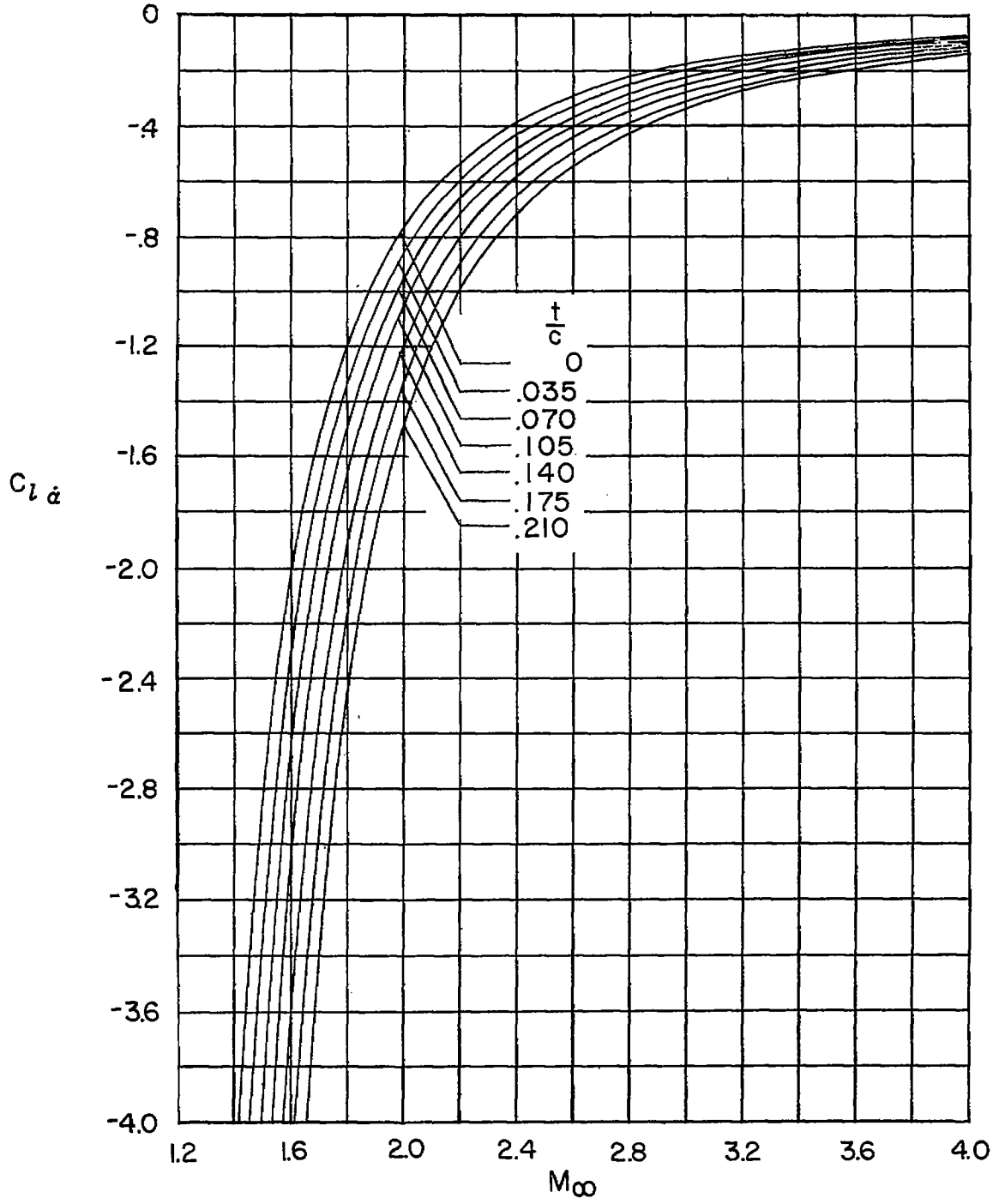

Figure 11.- Variation of c_{l_α} of a wedge airfoil for various thickness ratios. $\alpha_o = 0$.

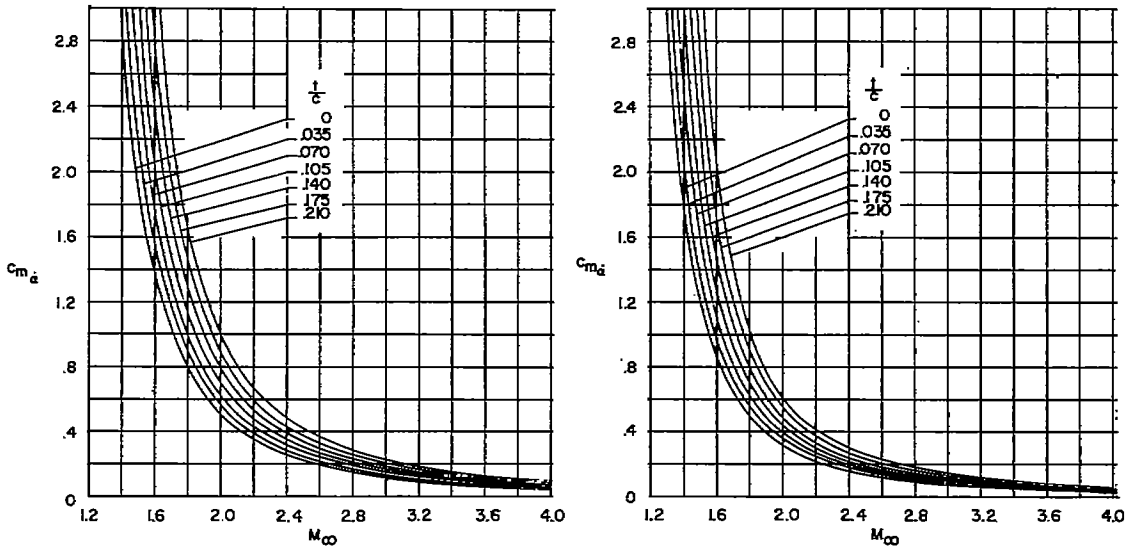

(a) $\xi = 0.$ (b) $\xi = 0.25.$

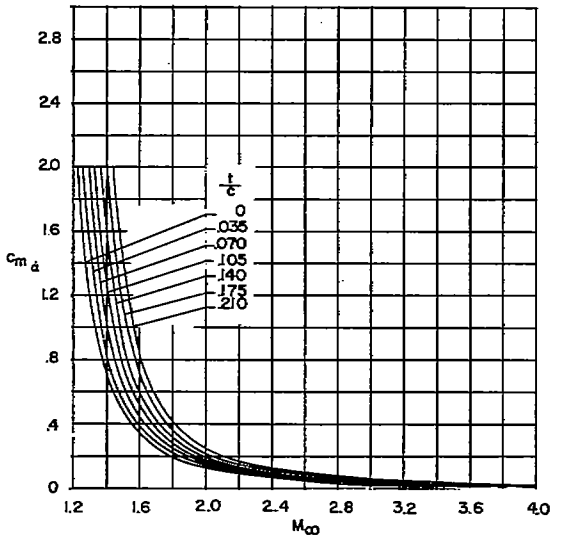

(c) $\xi = 0.50.$

Figure 12.- Variation of $c_{m_{\dot{\alpha}}}$ of a wedge airfoil with Mach number for various thickness ratios and pitch-axis locations. $\alpha_o = 0.$

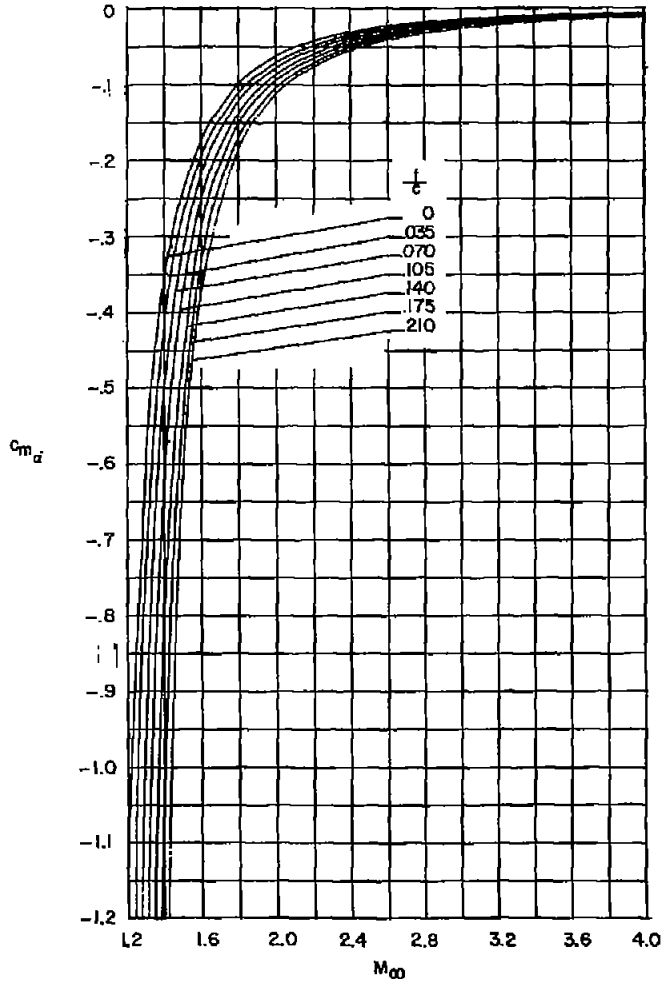

(d) $\xi = 0.75$.

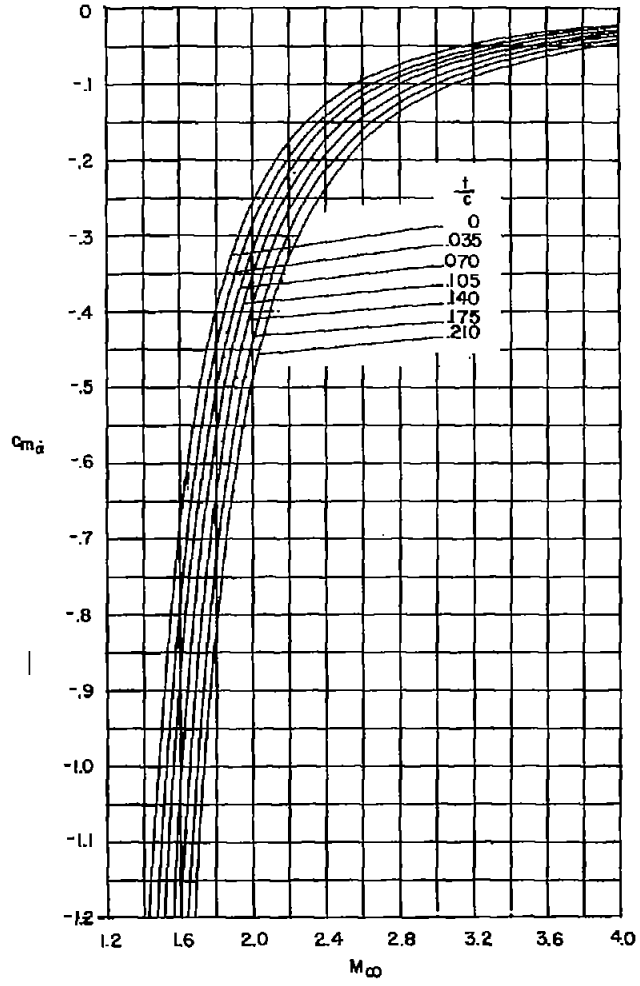

(e) $\xi = 1.00$.

Figure 12.- Concluded.

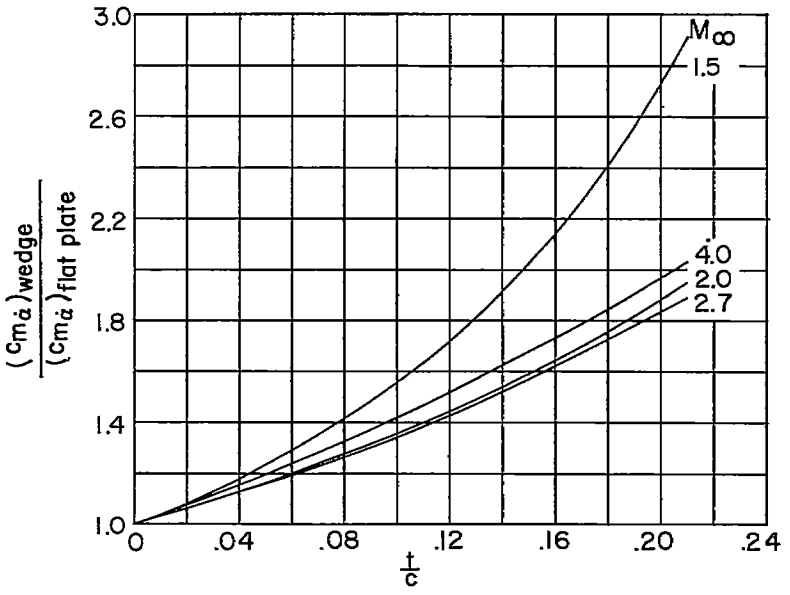

(a) $\xi = 0.25$.

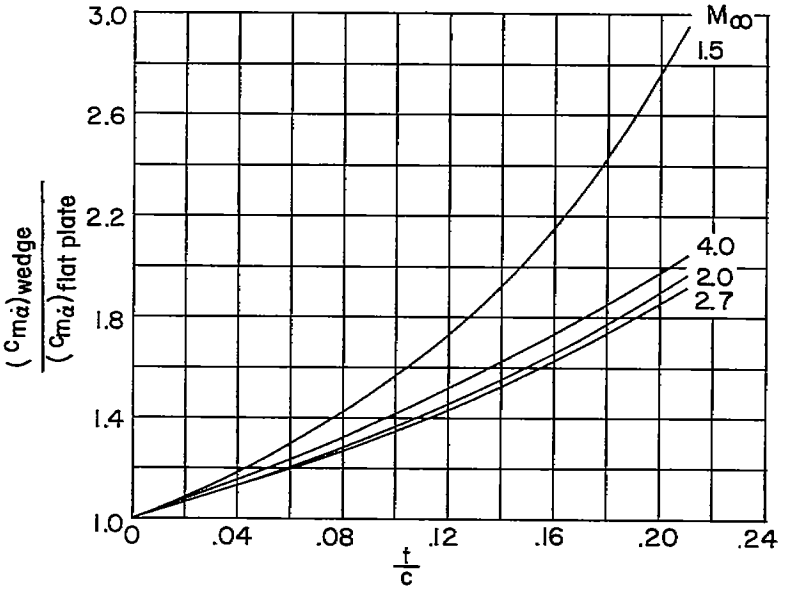

(b) $\xi = 0.50$.

Figure 13.- Effect of wedge thickness ratio on c_{m_α} for various free-stream Mach numbers. $\alpha_o = 0$.

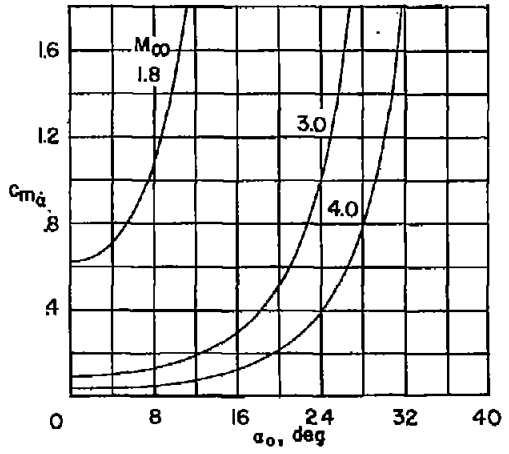

(a) $\xi = 0.25$; 7-percent-thick airfoil.

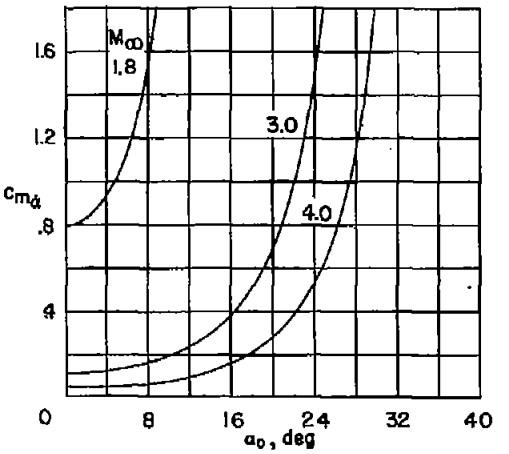

(b) $\xi = 0.25$; 14-percent-thick airfoil.

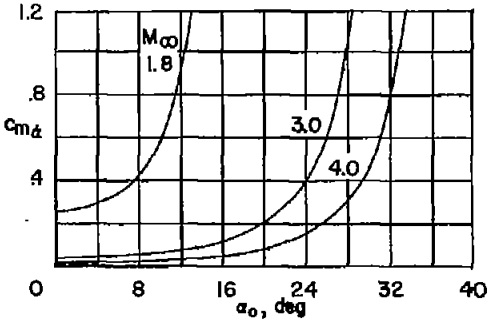

(c) $\xi = 0.50$; 7-percent-thick airfoil.

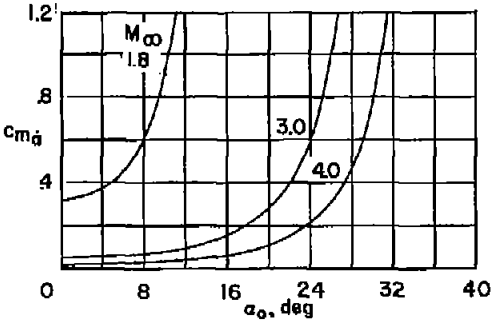

(d) $\xi = 0.50$; 14-percent-thick airfoil.

Figure 14.- Illustrative variation of $c_{m_{\dot{\alpha}}}$ of a wedge airfoil with angle of attack for various free-stream Mach numbers, wedge thicknesses, and pitch-axis locations.

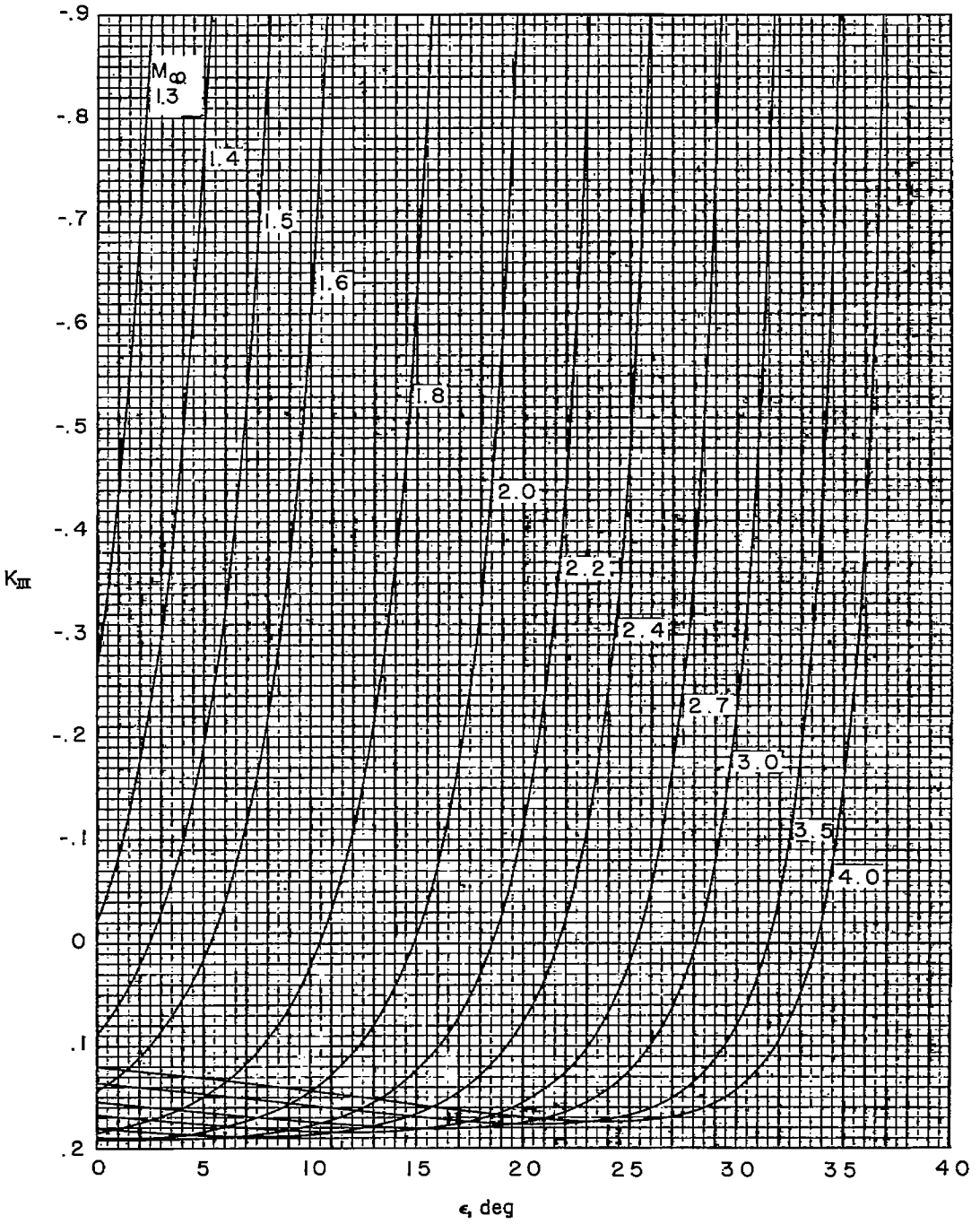

Figure 15.- Variation of K_{III} with ϵ for various free-stream Mach numbers.

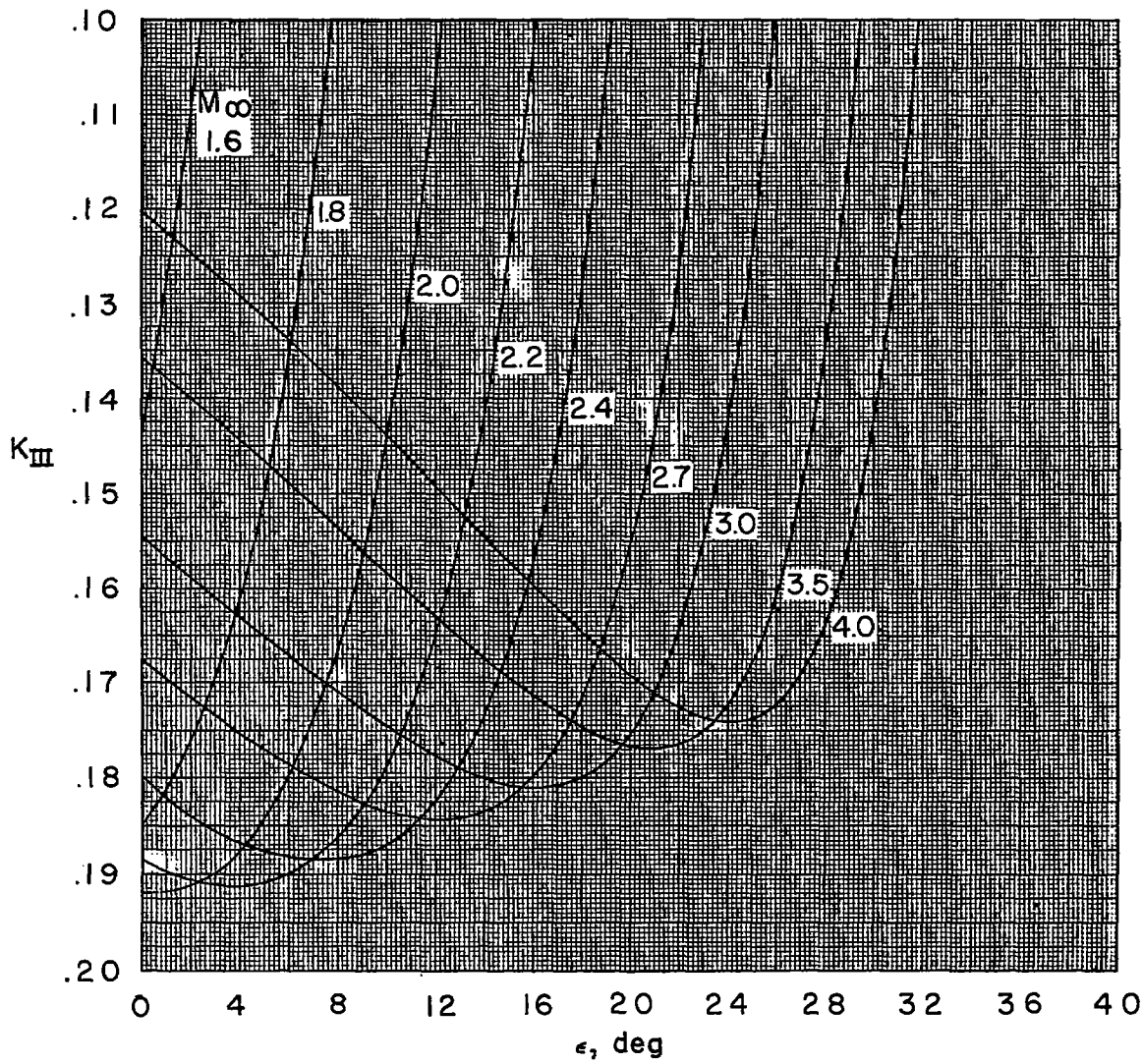

Figure 15.- Continued.

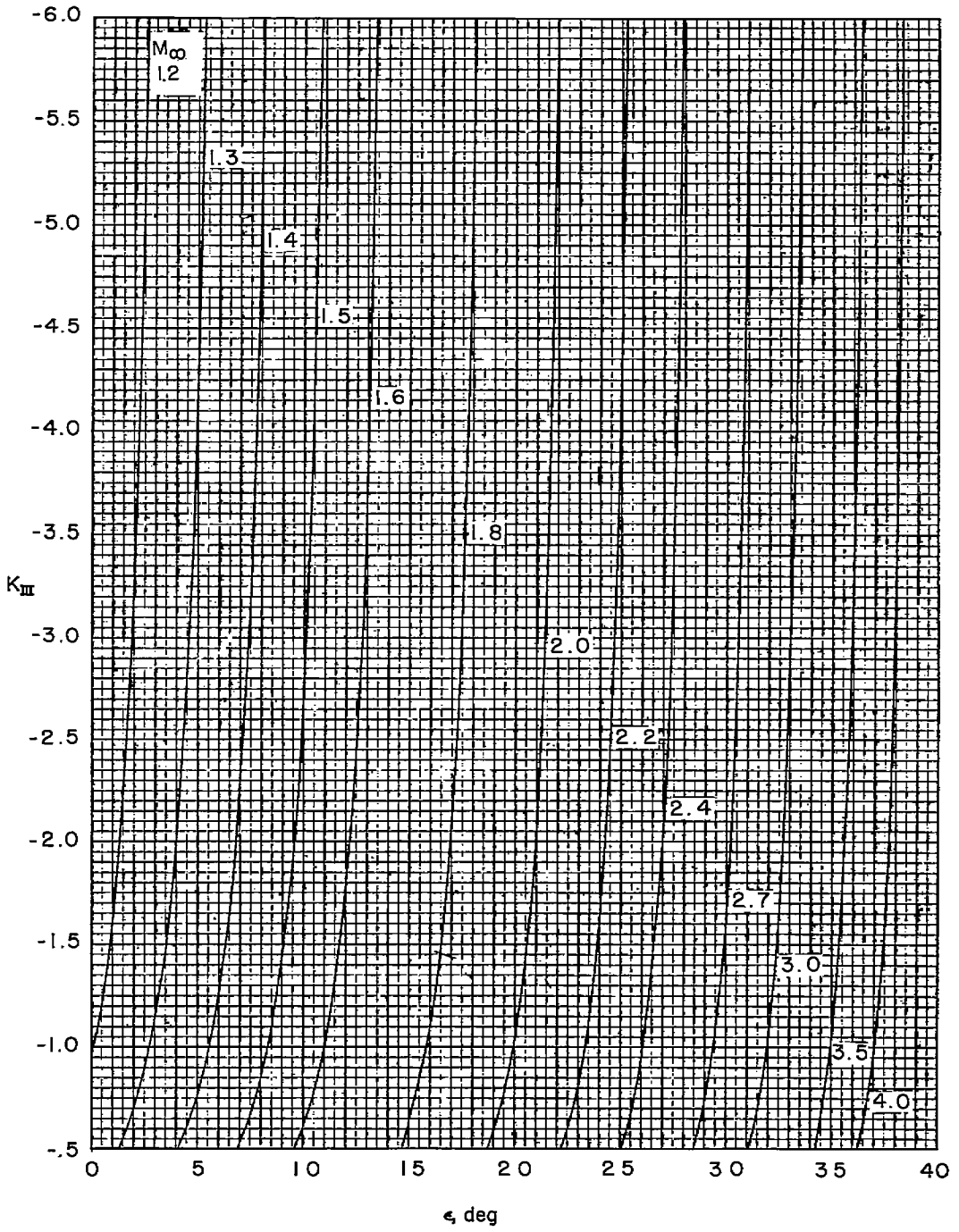

Figure 15.- Concluded.

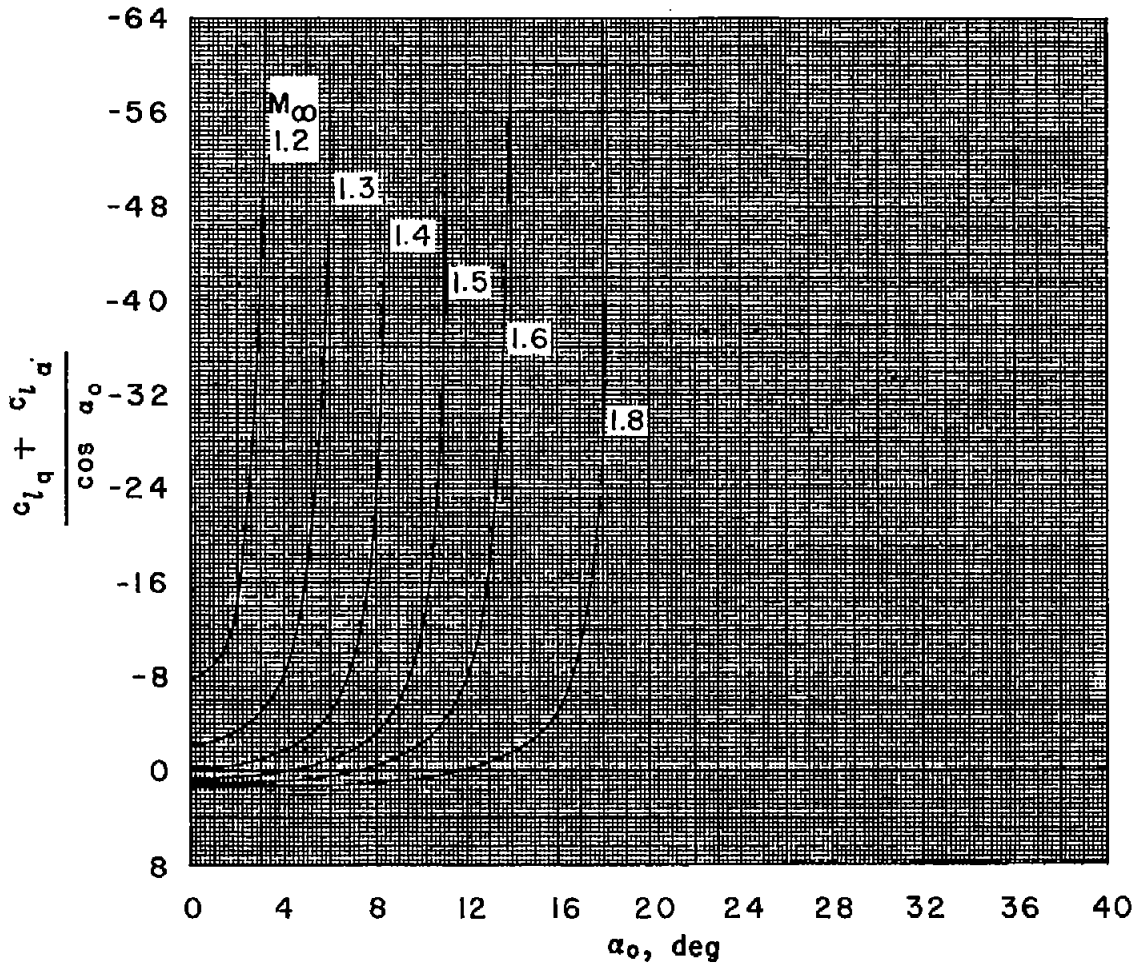

Figure 16.- Variation of $\frac{c_{l_q} + c_{l_{\dot{\alpha}}}}{\cos \alpha_o}$ with angle of attack for various free-stream Mach numbers.

$\xi = 0$.

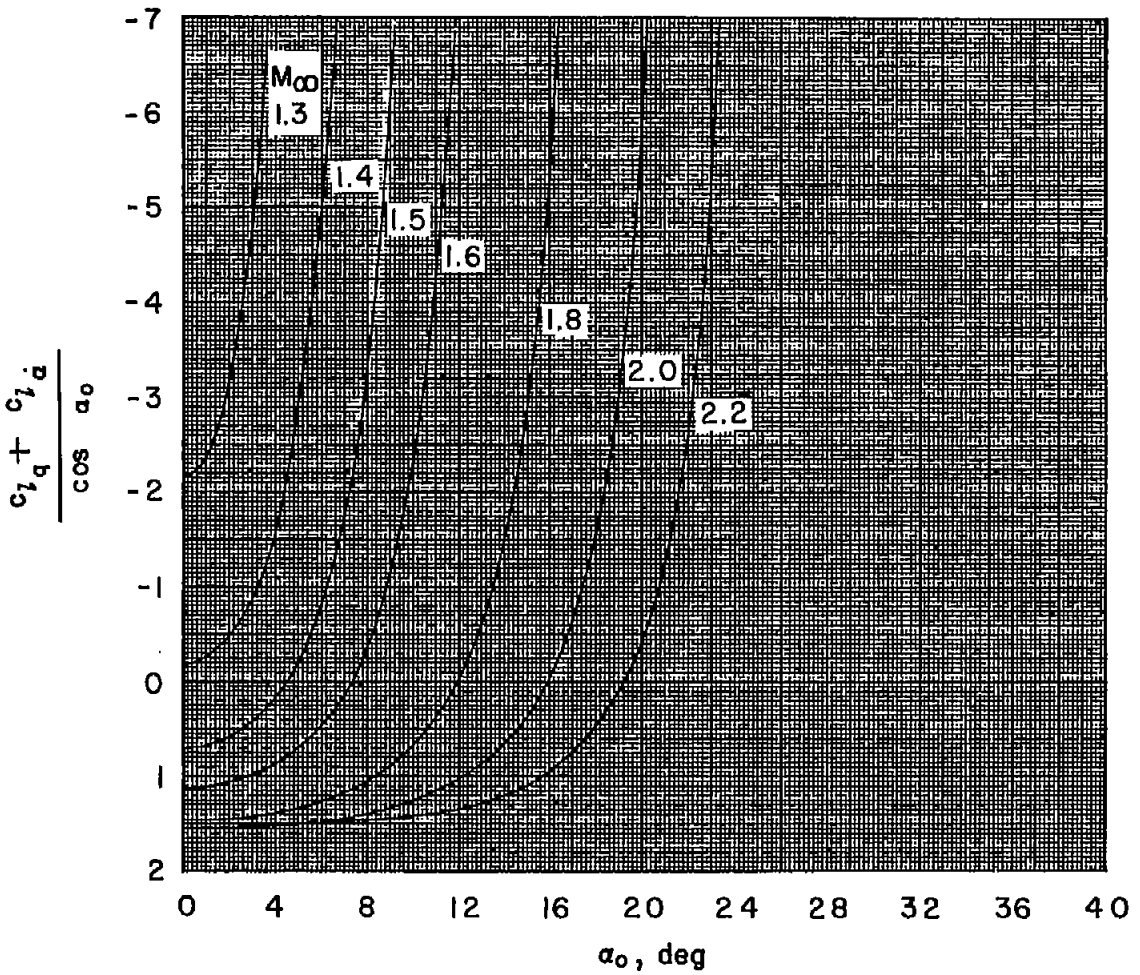

Figure 16.- Continued.

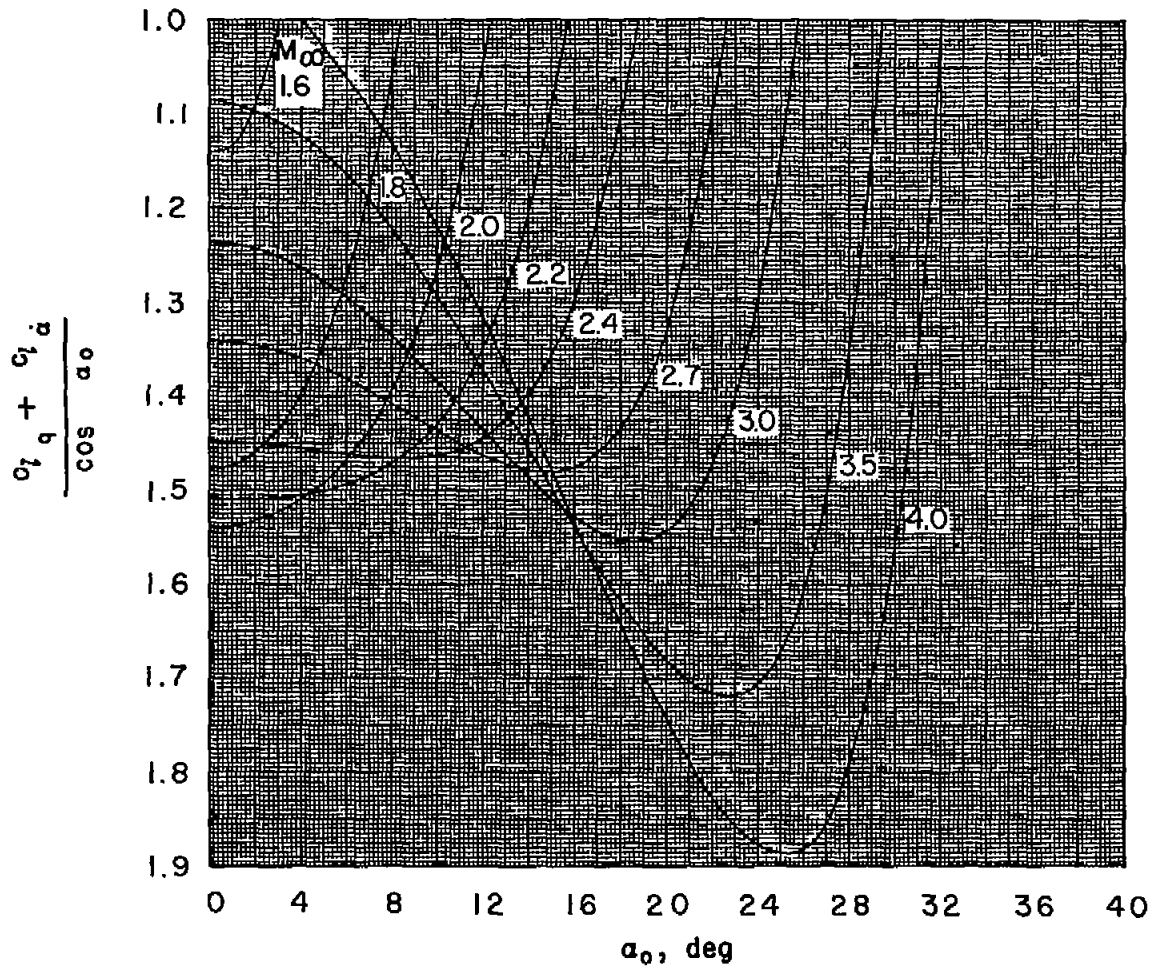

Figure 16.- Concluded.

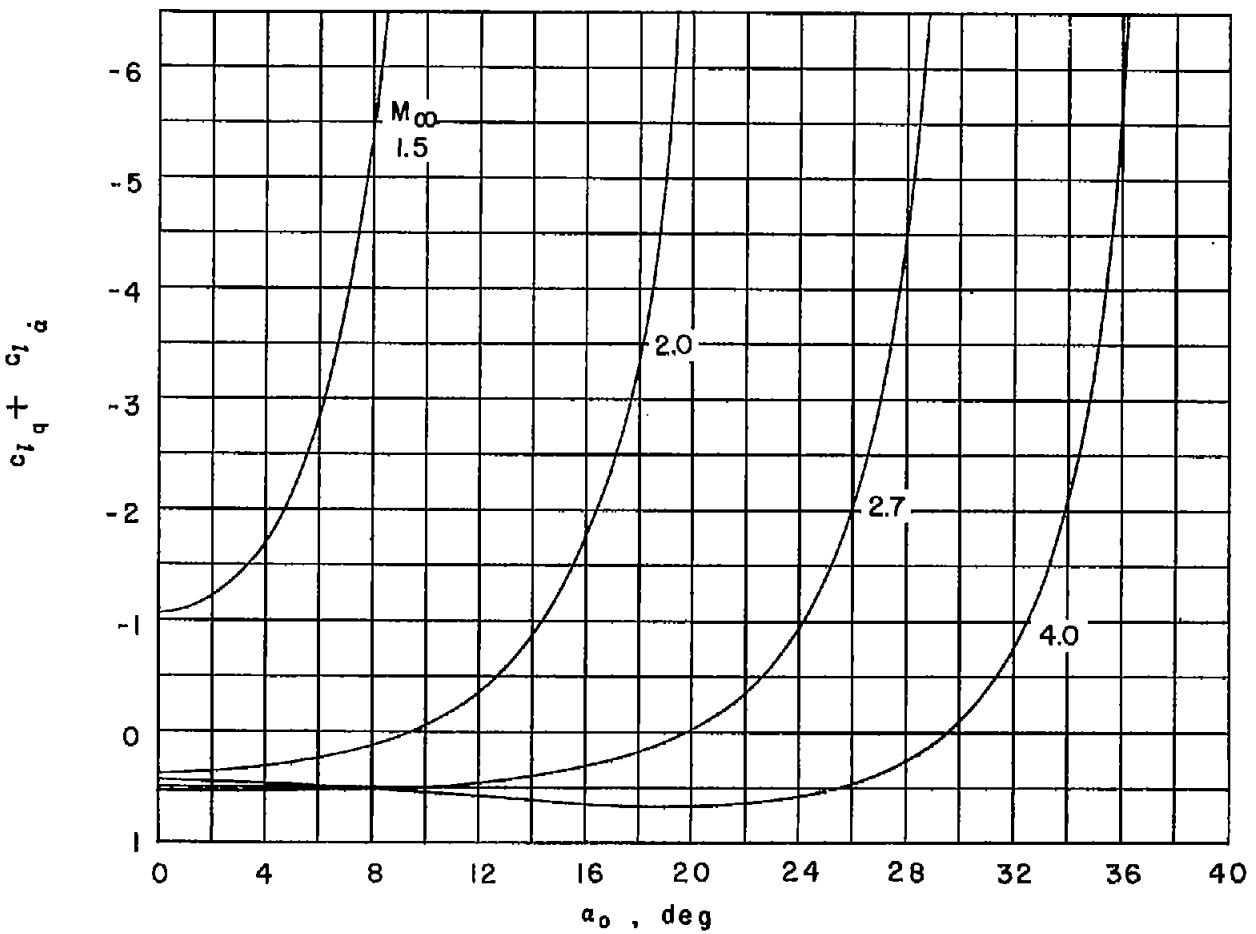

(a) $\xi = 0.25$.

Figure 17.- Illustrative variation of $c_{l_q} + c_{l_{\dot{\alpha}}}$ with angle of attack for various free-stream Mach numbers.

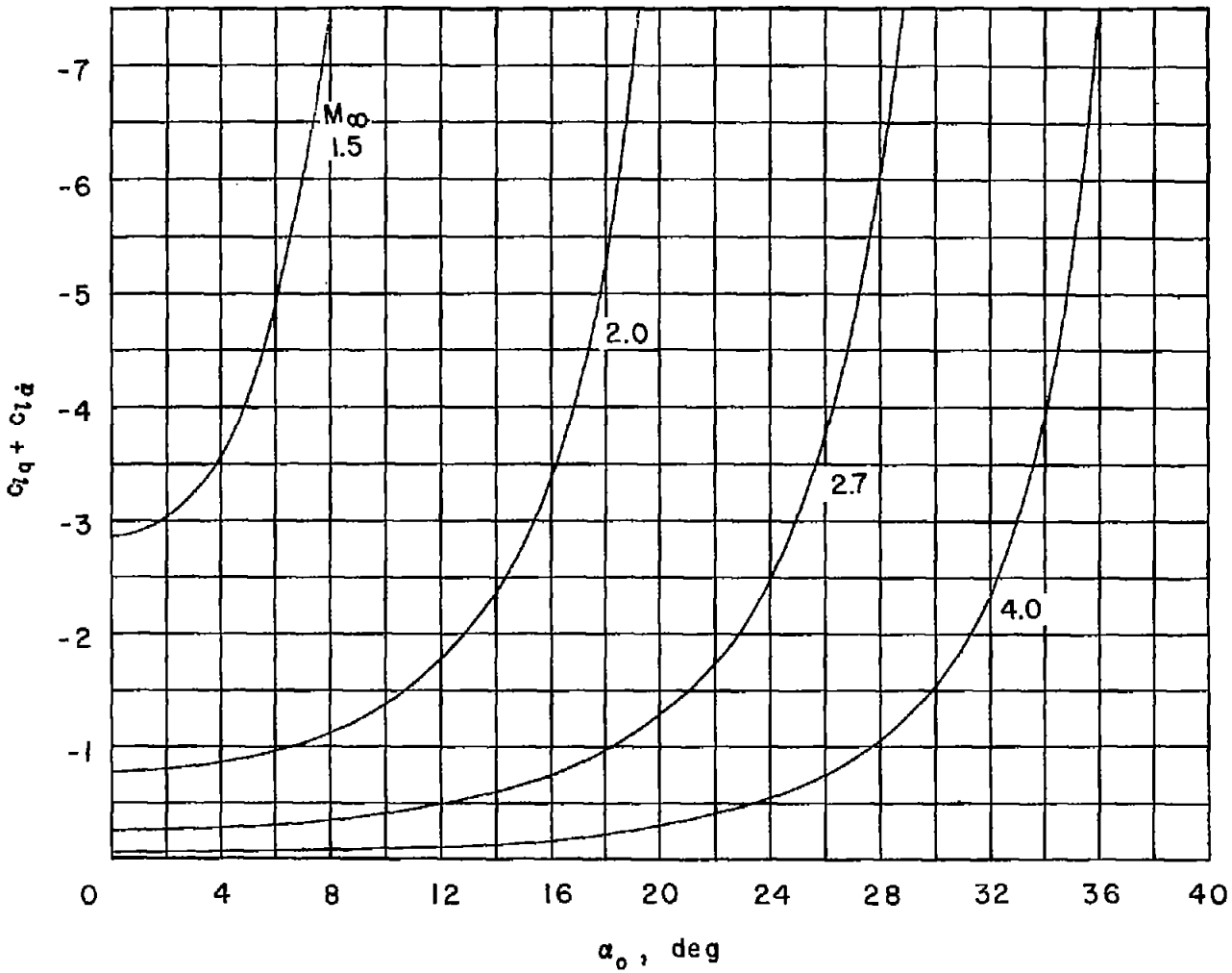

(b) $\xi = 0.50$.

Figure 17.- Concluded.

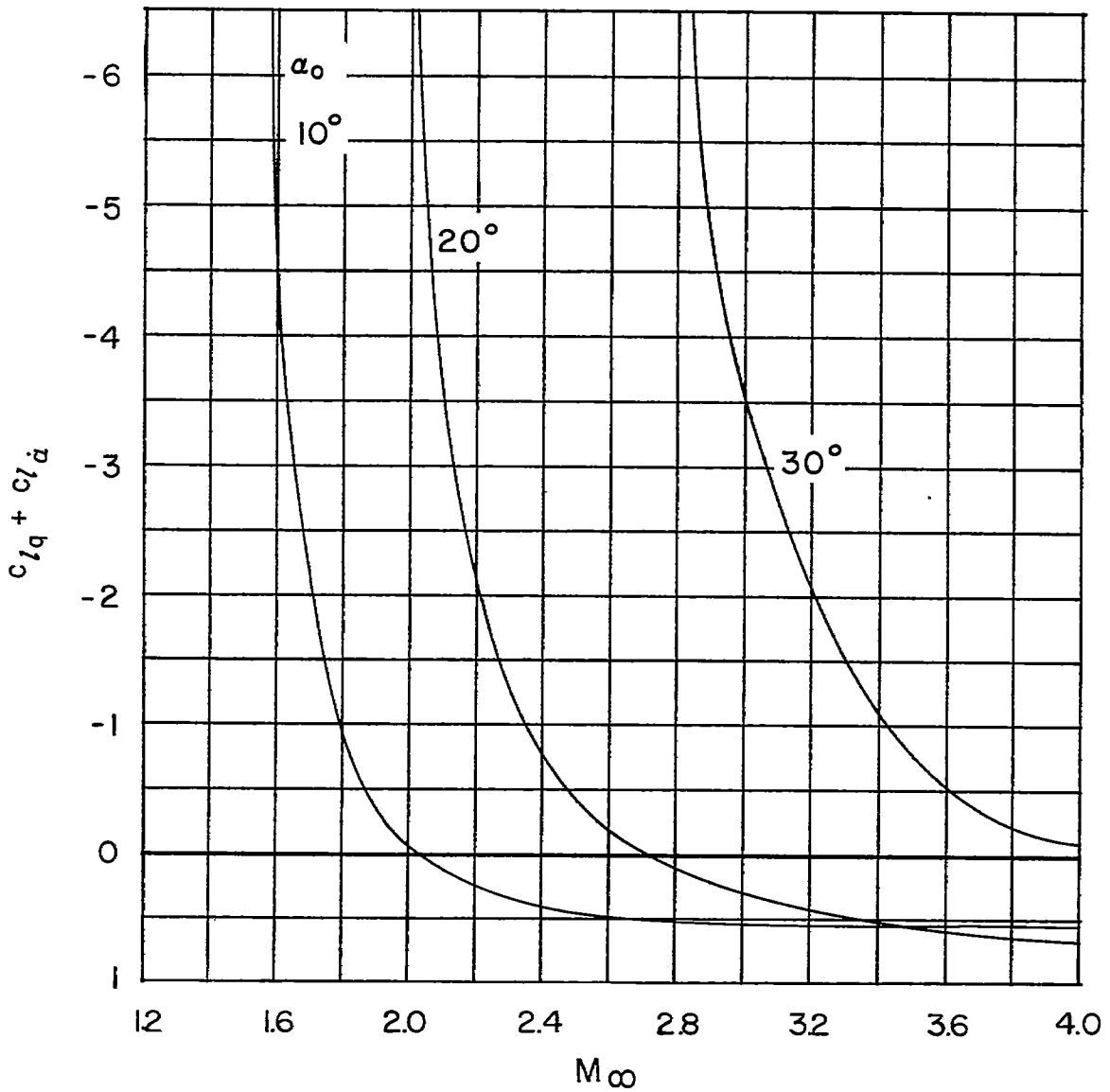

(a) $\xi = 0.25$.

Figure 18.- Illustrative variation of $c_{l_q} + c_{l_{\dot{\alpha}}}$ with free-stream Mach number for various angles of attack.

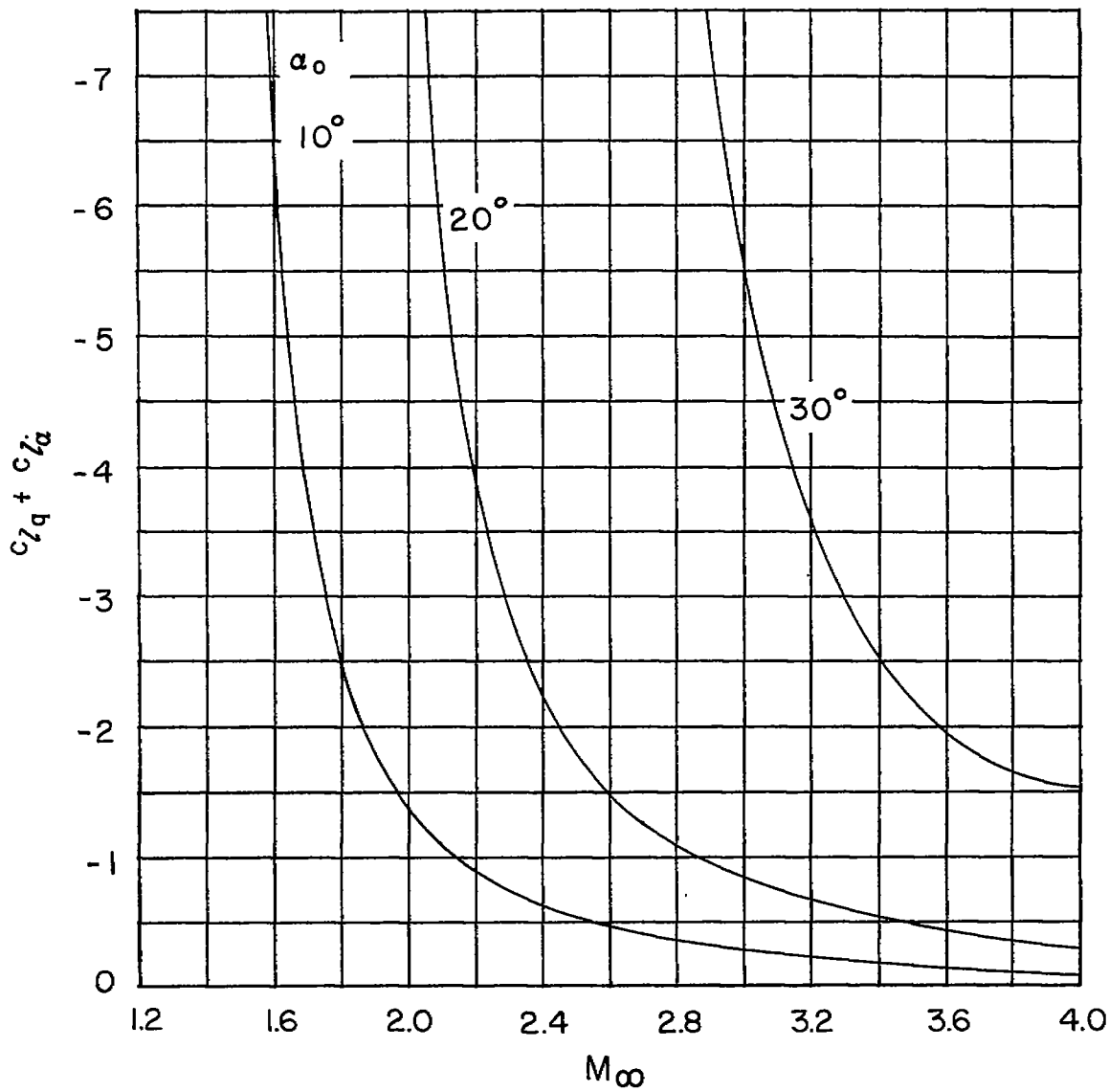

(b) $\xi = 0.50$.

Figure 18.- Concluded.

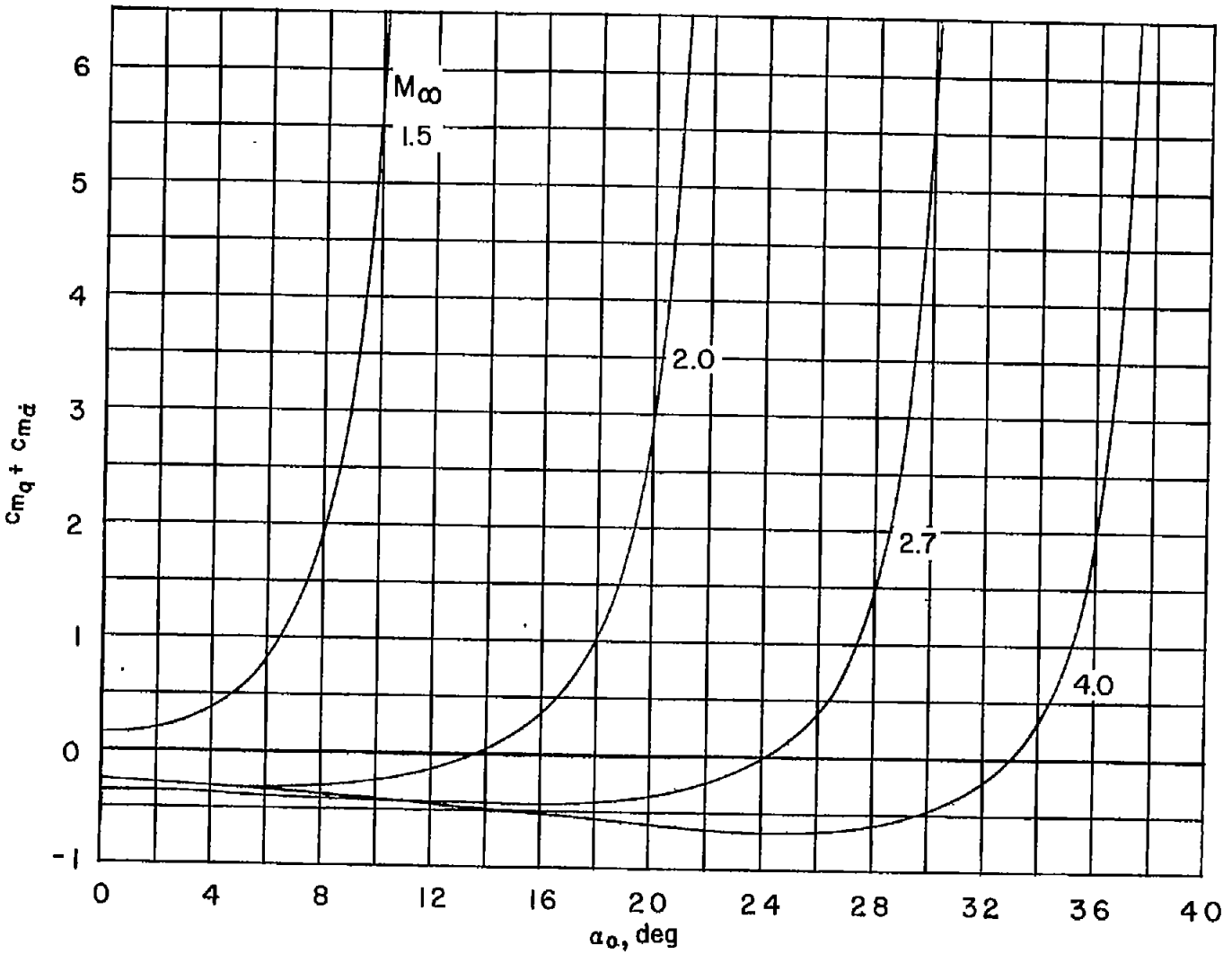

(a) $\xi = 0.25$.

Figure 19.- Illustrative variation of $c_{m_q} + c_{m_{\dot{\alpha}}}$ with angle of attack for various free-stream Mach numbers.

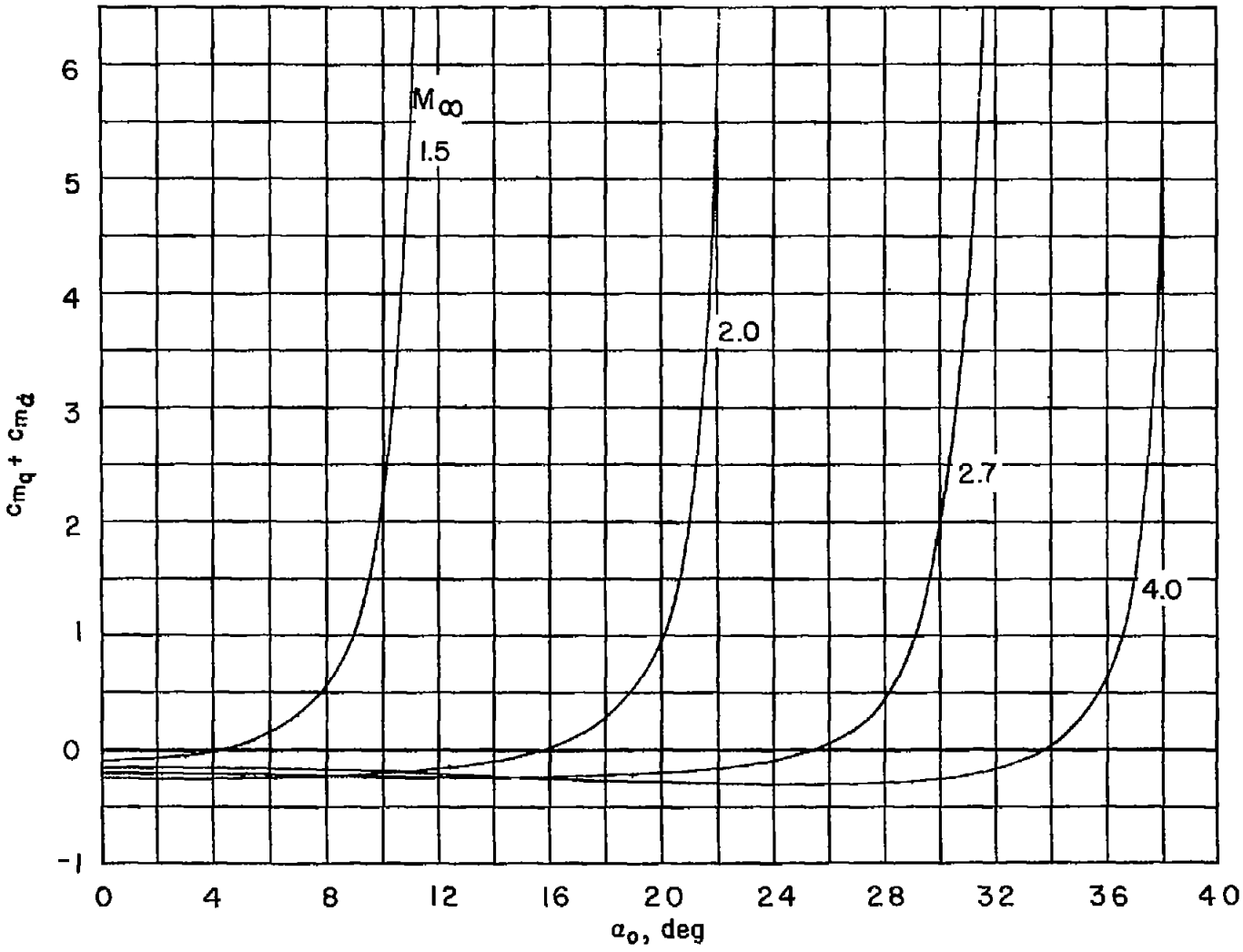

(b) $\xi = 0.50$.

Figure 19.- Concluded.

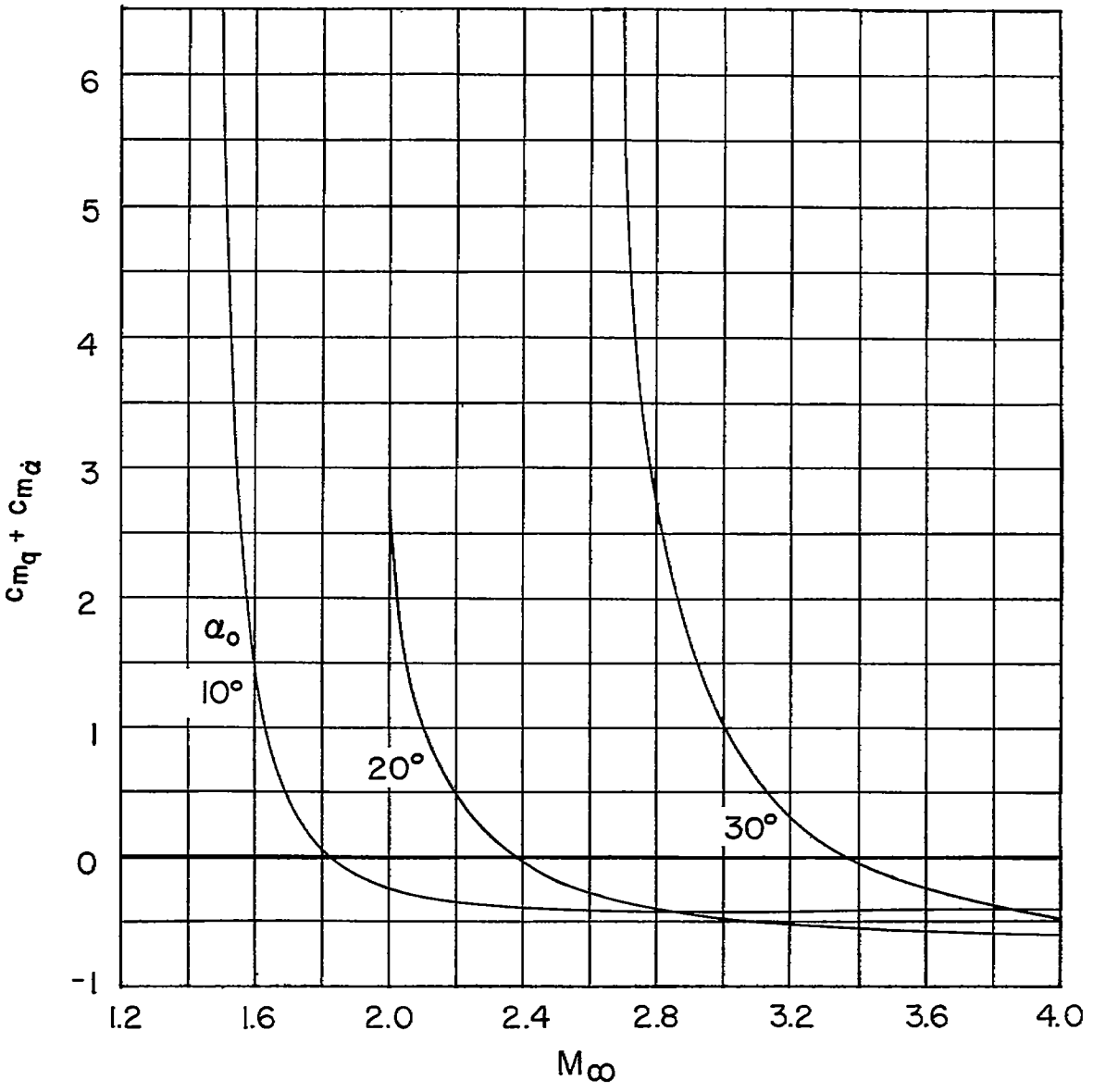

(a) $\xi = 0.25$.

Figure 20.- Illustrative variation of $c_{m_q} + c_{m_{\dot{\alpha}}}$ with free-stream Mach number for various angles of attack.

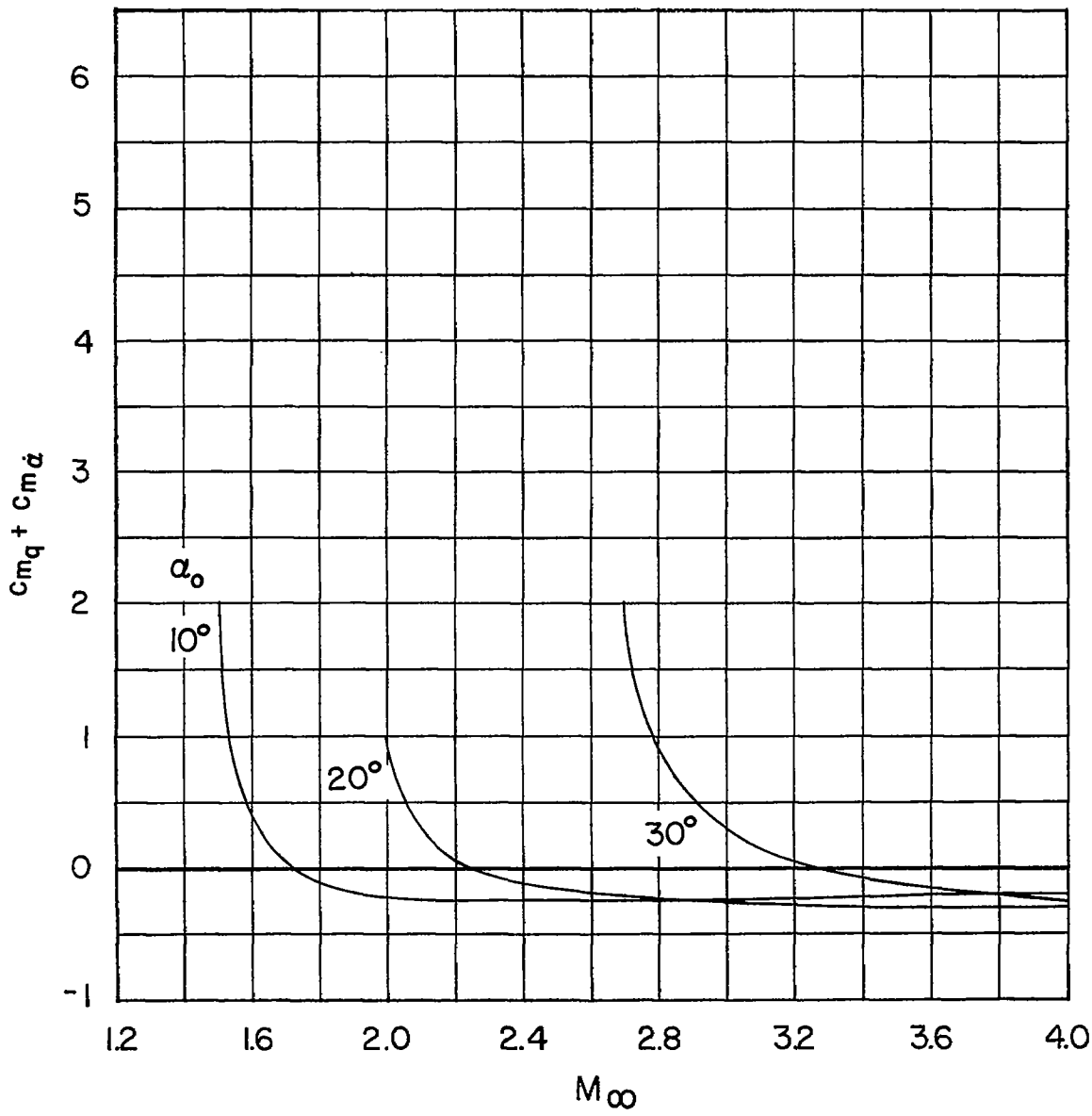

(b) $\xi = 0.50$.

Figure 20.- Concluded.

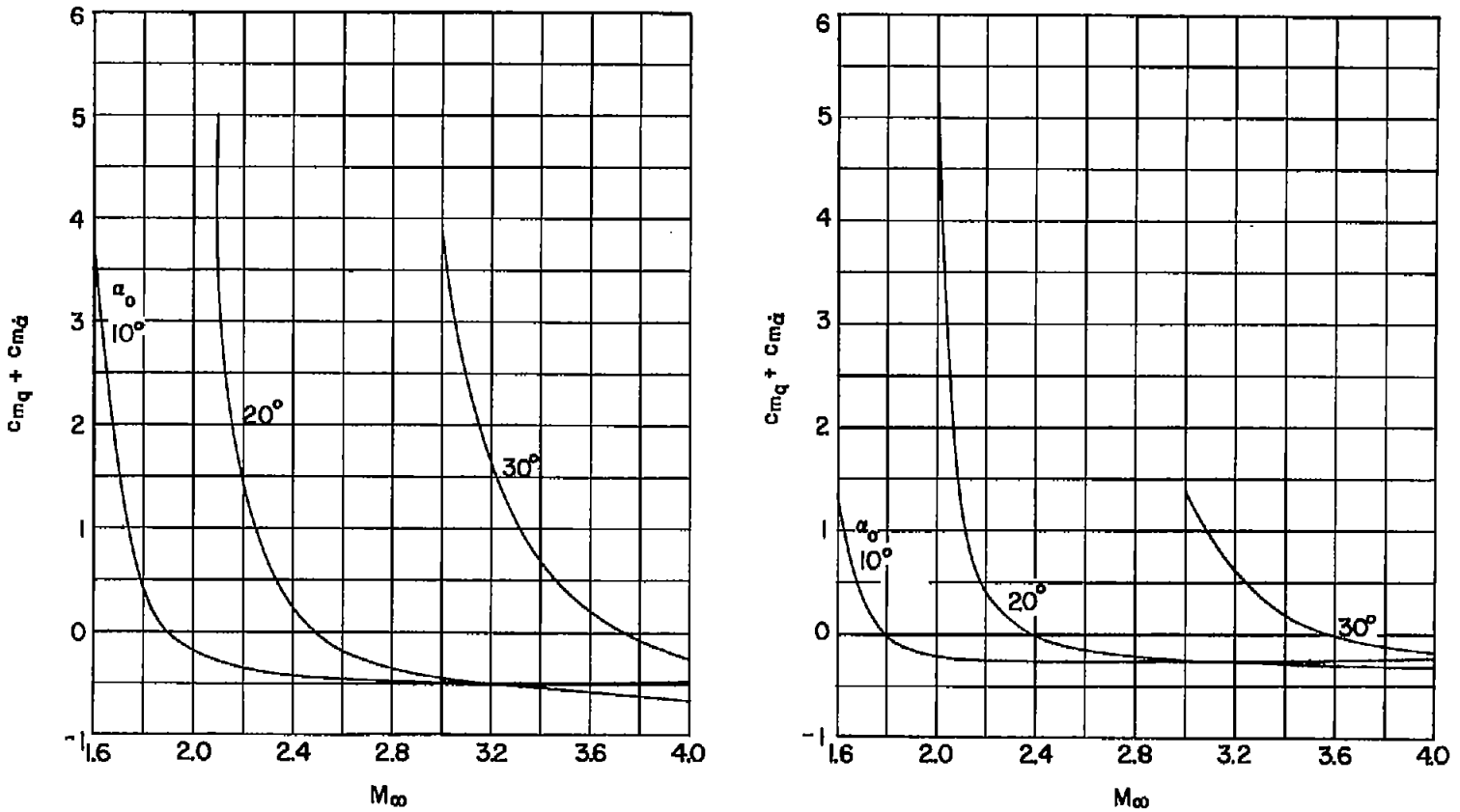

(a) $\xi = 0.25$.

(b) $\xi = 0.50$.

Figure 21.- Illustrative variation of $c_{m_q} + c_{m_{\dot{\alpha}}}$ of a 7-percent-thick wedge airfoil with free-stream Mach number for various angles of attack.

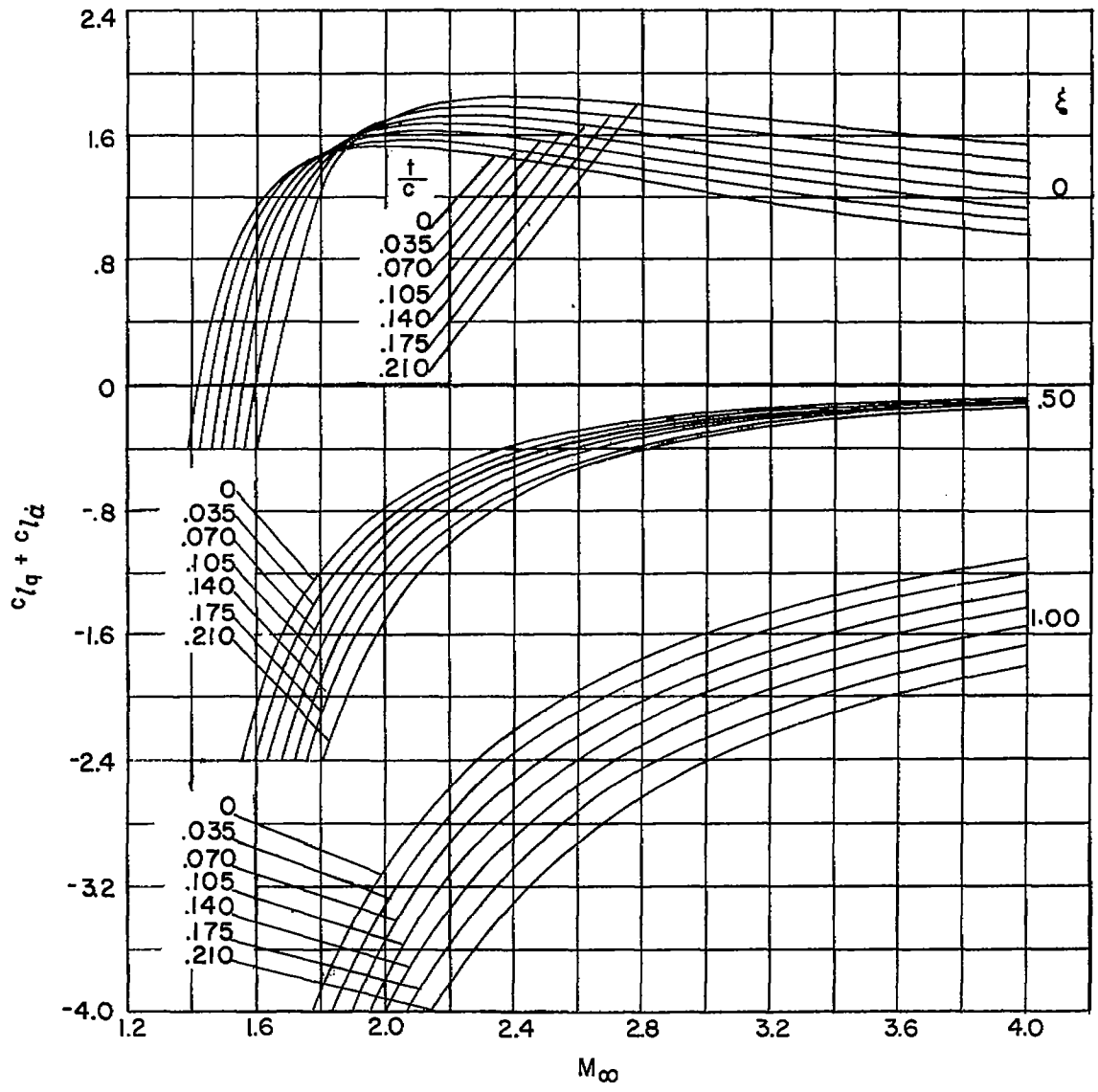

Figure 22.- Illustrative variation of $c_{l_q} + c_{l_{\dot{\alpha}}}$ of a wedge airfoil with free-stream Mach number for various thickness ratios and pitch-axis locations. $\alpha_o = 0$.

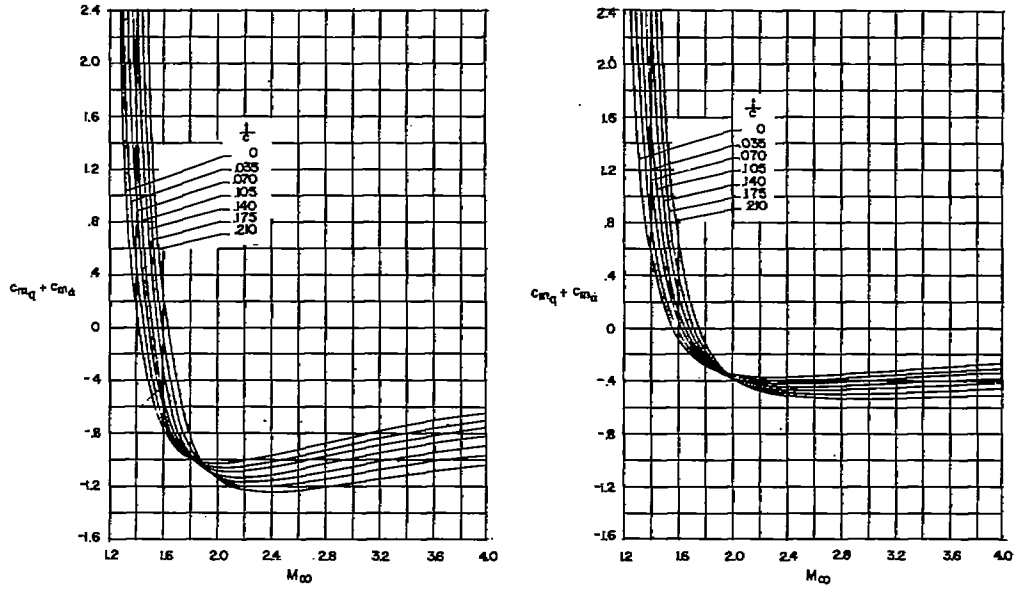

(a) $\xi = 0.$ (b) $\xi = 0.25.$

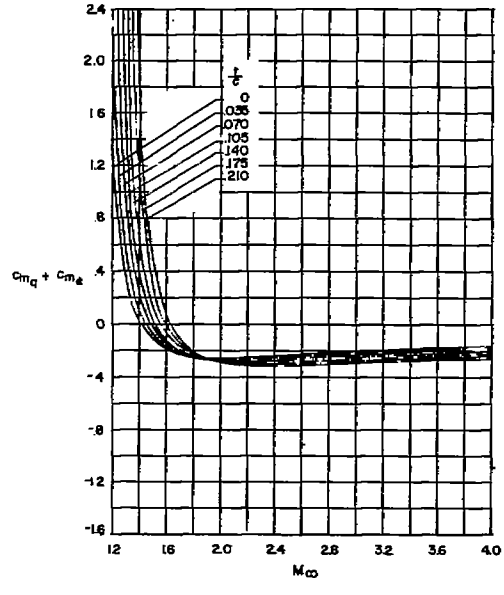

(c) $\xi = 0.50.$

Figure 23.- Illustrative variation of $c_{m_q} + c_{m_{\dot{\alpha}}}$ of a wedge airfoil with free-stream Mach number for various wedge locations. $\alpha_o = 0.$

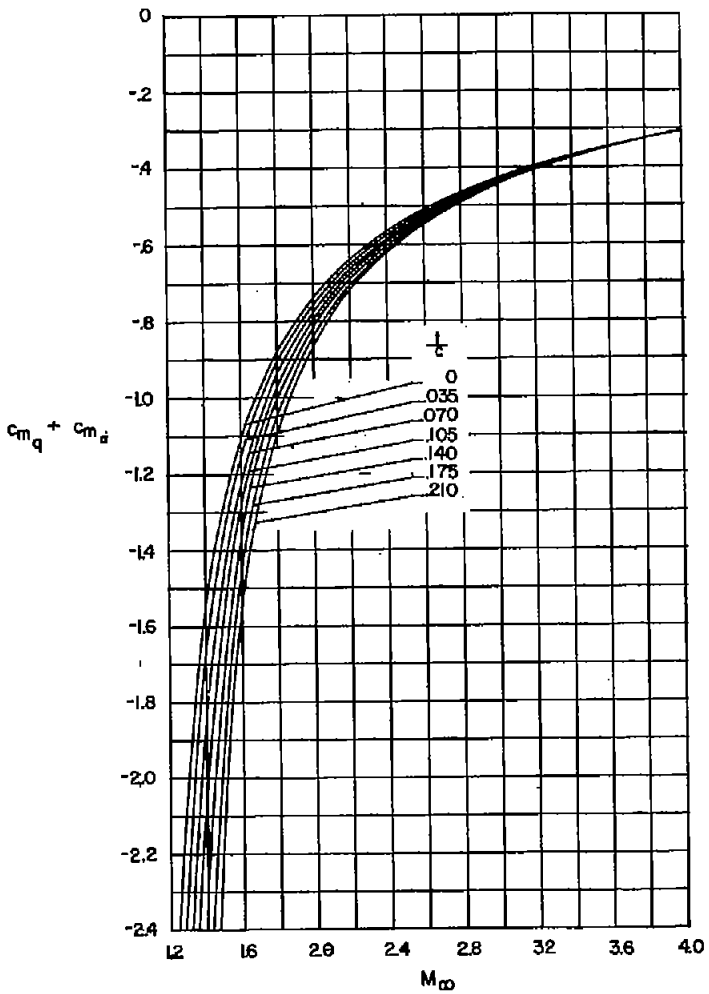

(d) $\xi = 0.75$.

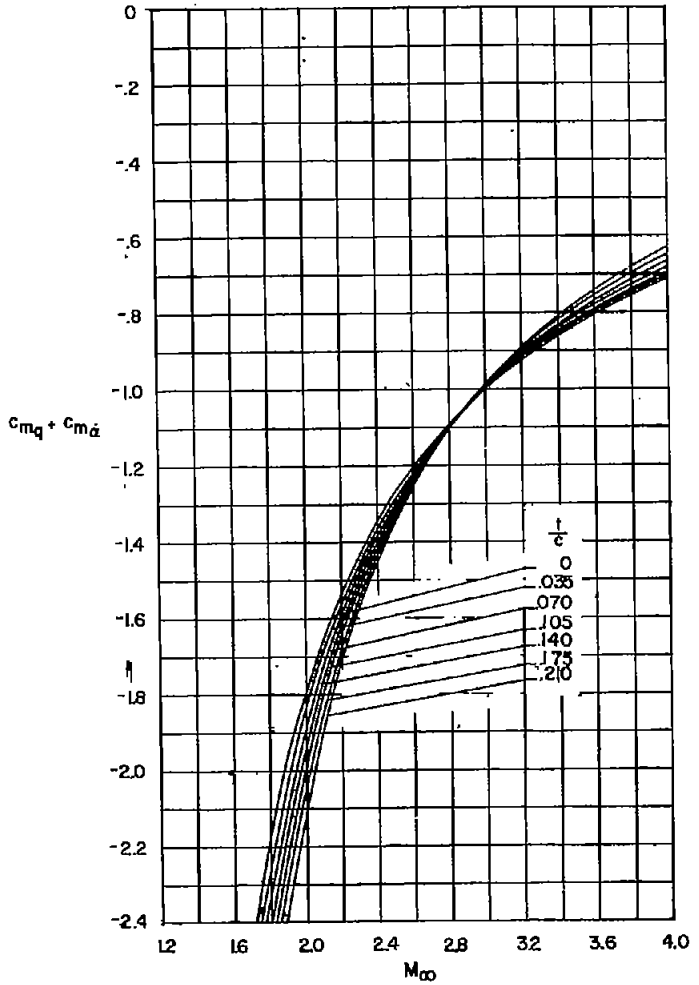

(e) $\xi = 1.00$.

Figure 23.- Concluded.

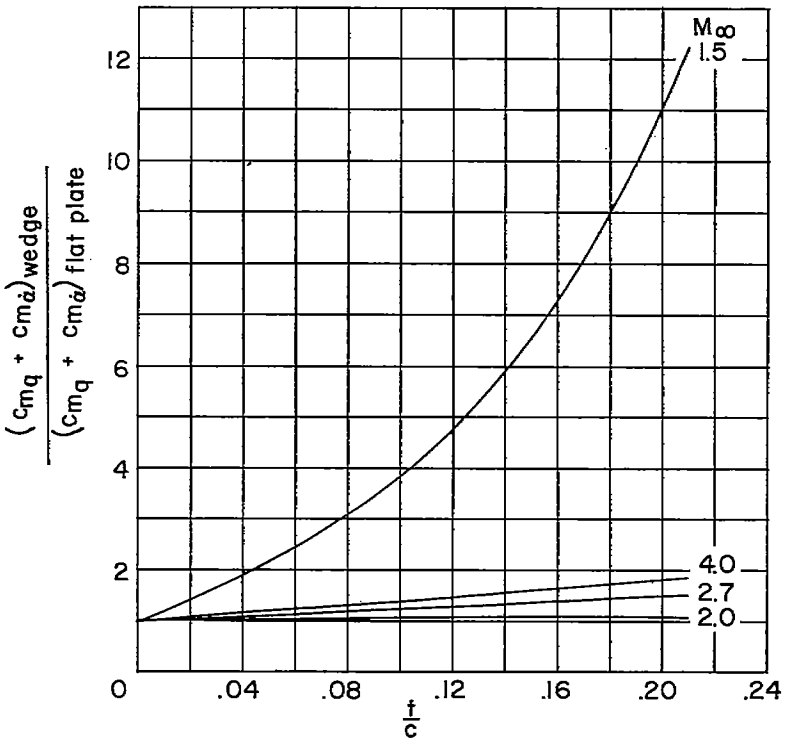

(a) $\xi = 0.25$.

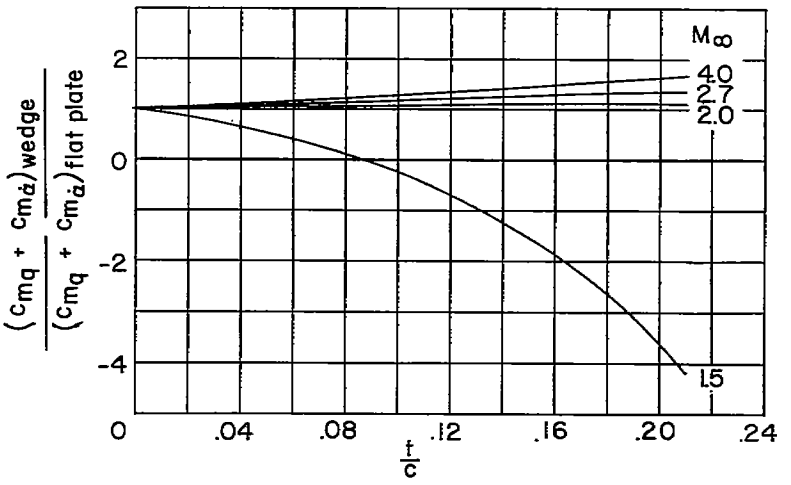

(b) $\xi = 0.50$.

Figure 24.- Effect of wedge thickness on $c_{m_q} + c_{m_{\dot{\alpha}}}$ for various thickness ratios and pitch-axis locations. $\alpha_o = 0$.

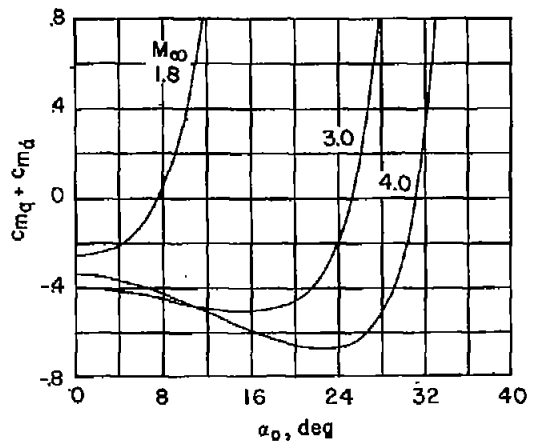

(a) $\xi = 0.25$; 7-percent-thick airfoil.

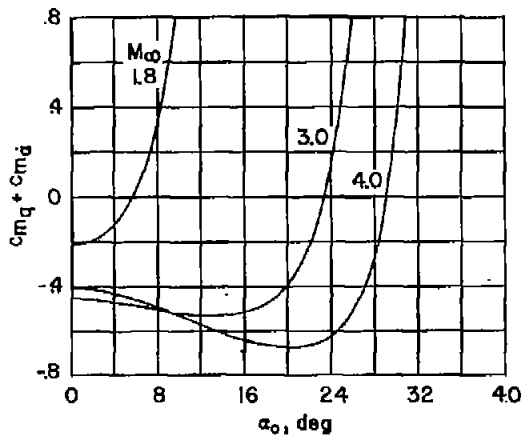

(b) $\xi = 0.25$; 14-percent-thick airfoil.

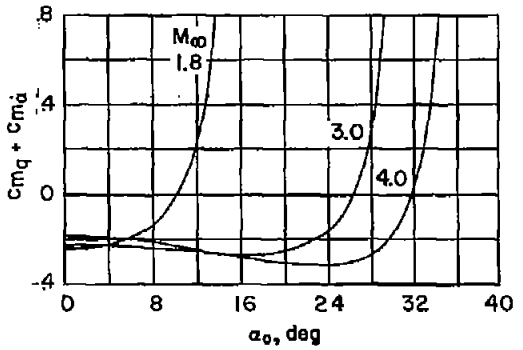

(c) $\xi = 0.50$; 7-percent-thick airfoil.

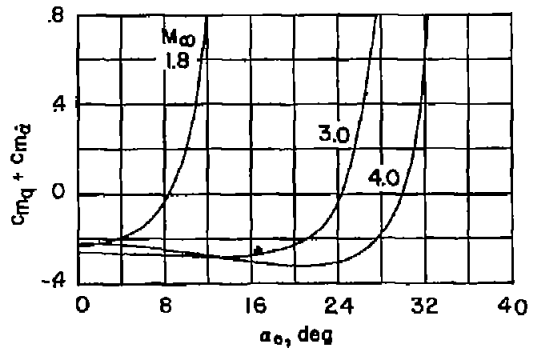

(d) $\xi = 0.50$; 14-percent-thick airfoil.

Figure 25.- Illustrative variation of $c_{m_q} + c_{m_{\dot{\alpha}}}$ of a wedge airfoil with angle of attack for various free-stream Mach numbers, wedge thicknesses, and pitch-axis locations.

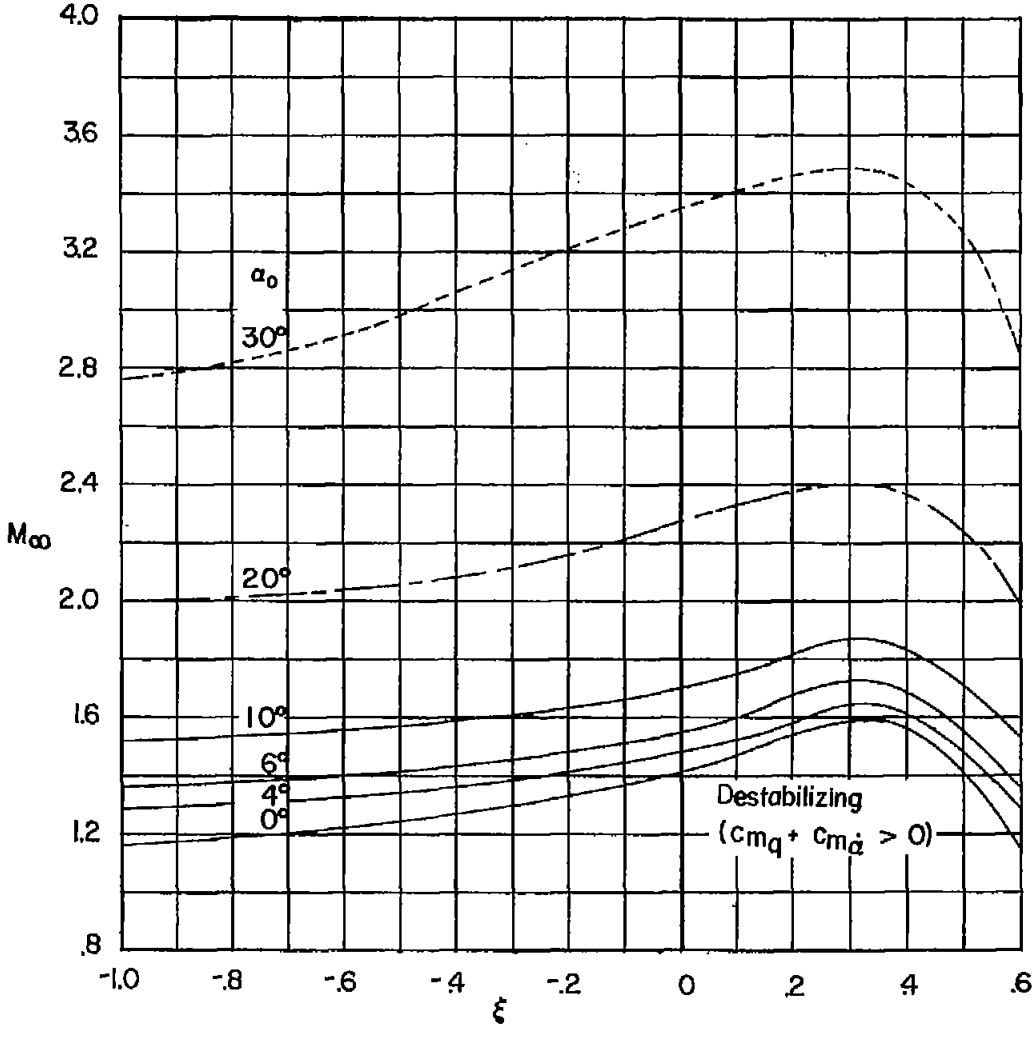

Figure 26.- Effect of angle of attack on boundary of neutral stability for a flat-plate airfoil. $c_{m_q} + c_{m_{\dot\alpha}} = 0$.

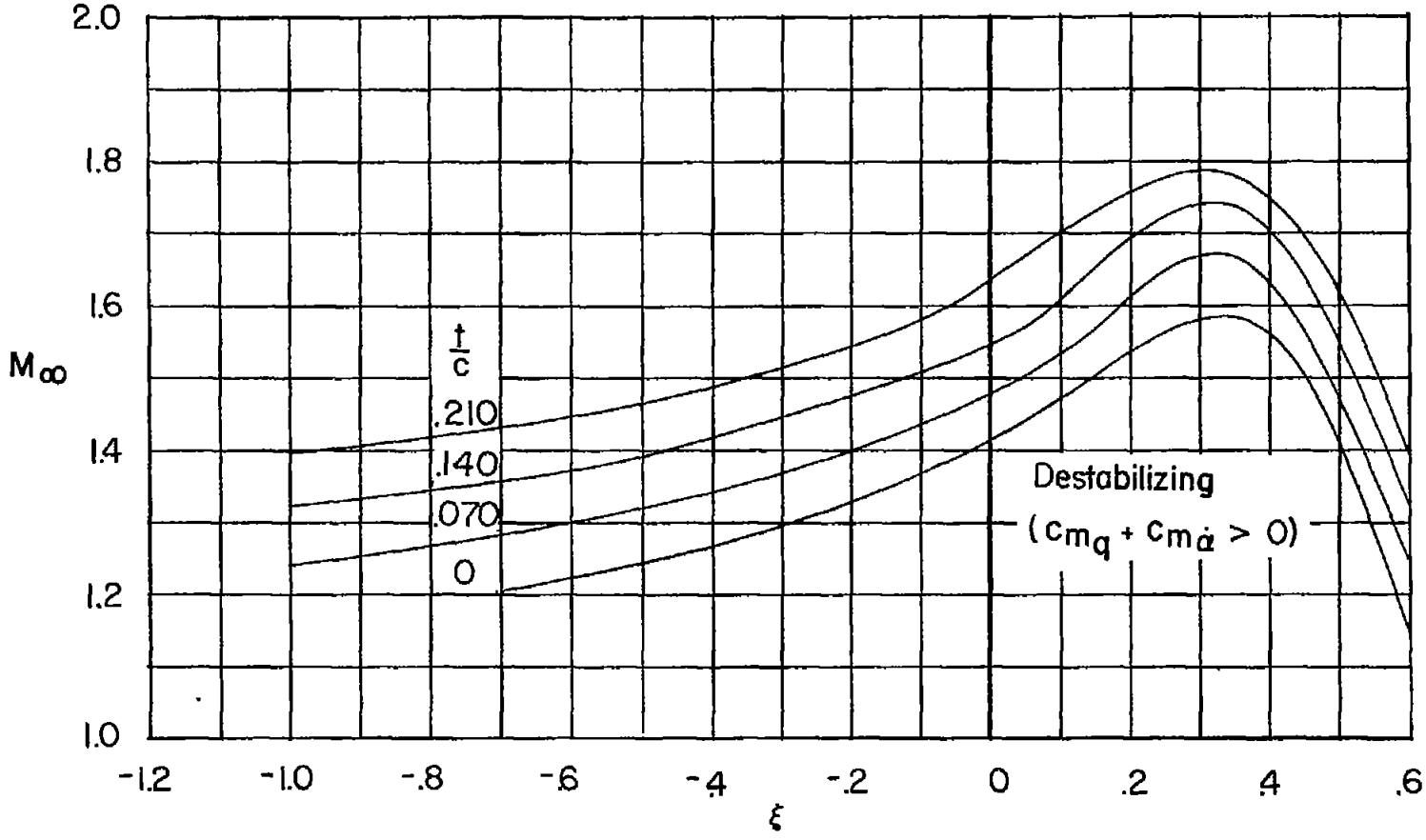

Figure 27.- Effect of wedge thickness on boundary of neutral stability. $c_{m_q} + c_{m_{\dot{\alpha}}} = 0$.

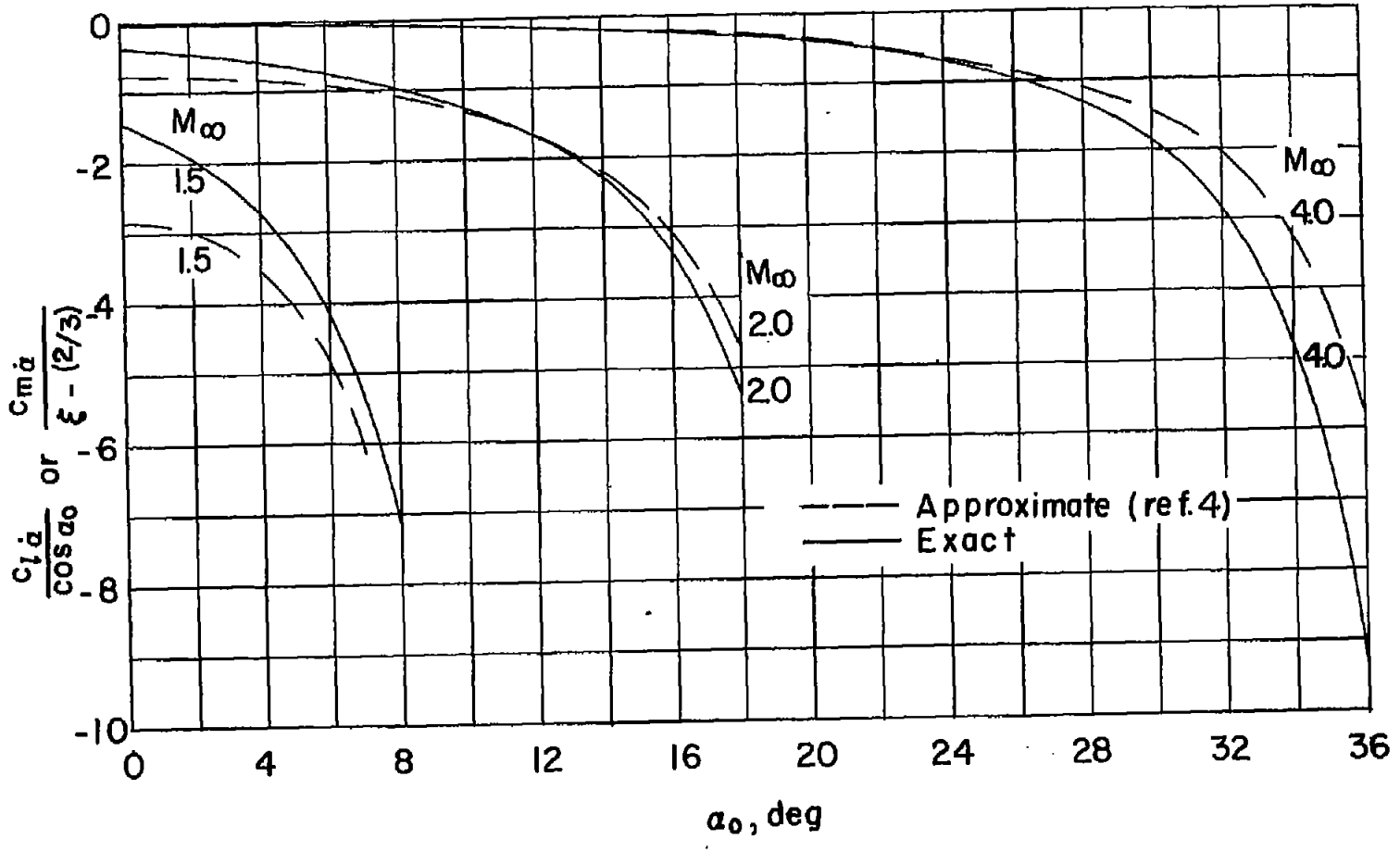

Figure 28.- Comparison of approximate and exact values of $\frac{c_{l_\dot{\alpha}}}{\cos \alpha_o}$ $\left(\text{or } \frac{c_{m_\dot{\alpha}}}{\xi - 2/3}\right)$.